This is to certify that the

thesis entitled

PREDICTION OF SHEAR INDUCED ENZYME

ACTIVITY LOSS IN FLOW SYSTEMS

presented by

Carl Robert Beck

has been accepted towards fulfillment
of the requirements for

___Ph. D.___ degree in _Chemical Engineering_

Donald K. M. Anderson
Major professor

Date _7/4/79_

O-7639

PREDICTION OF SHEAR INDUCED ENZYME

ACTIVITY LOSS IN FLOW SYSTEMS

By

Carl Robert Beck

A DISSERTATION

Submitted to
Michigan State University
in partial fulfillment of the requirements
for the degree of

DOCTOR OF PHILOSOPHY

Department of Chemical Engineering

1979

ABSTRACT

PREDICTION OF SHEAR INDUCED ENZYME

ACTIVITY LOSS IN FLOW SYSTEMS

By

Carl Robert Beck

The exceptional catalytic potential of enzymes for industrial processes is limited by their fragile nature. This fragile nature is exemplified by a loss of catalytic activity in shear fields. Bovine liver catalase was used as a model system to study this effect in a stirred tank and in a Couette viscometer and this enzyme was found to have an activation energy of approximately 7 kcal/gmole for the "degradation" reaction. This suggests that the mechanism for enzyme damage in shear flow may be the breaking of one or two hydrogen bonds in the quaternary structure of the enzyme.

A method is proposed here to predict the enzyme activity loss one might expect in industrial flow processes. The method requires the rate of activity loss of the proposed enzyme solution at a fixed shear rate to be measured experimentally in a viscometer. From this data, an activation energy and a frequency factor of degradation are calculated which relate the degradation rate to shear stress and temperature. This relationship is combined with a function describing the distribution of shear in the proposed process to predict the rate of activity loss in that process.

A shear distribution function F is defined such that Fds is the fraction of fluid in the vessel which is experiencing a shear rate

between s and s+ds. Then the rate of degradation of enzyme in this volume fraction becomes

$$R_s \; F ds \qquad\qquad (1)$$

where R_s is the rate of deactivation of enzyme experiencing a shear rate s, which must be determined experimentally. The total rate of deactivation is found by integrating over all shear rates

$$R_t = \int_0^\infty R_s \; F \; ds \qquad\qquad (2)$$

The shear distribution function is unknown for many important flow systems, such as the baffled stirred tank used in this study. Since the shear distribution function for such a process cannot be rigorously defined, several trial functions are examined: for Model 1, it is assumed that most of the fluid in the tank is being sheared at a high rate; for Model 2 any shear rate (from zero up to a maximum value) is assumed equally likely; in Model 3 most of the fluid in the tank is under low shear; and for Model 4 the shear rate decays exponentially with distance from the center of the tank. These four models were used, along with enzyme degradation data from a viscometer to derive an equation which predicts the rate of degradation in a stirred tank, as follows

$$R_t = KZ_v(P\mu/V)^{1/2}a \qquad\qquad (3)$$

where K is a constant which depends on the form of the shear distribution function, P is the power input to the fluid, μ is the viscosity, Z_v is a parameter obtainable from measurements in a constant shear viscometer, and a is the concentration of active enzyme present. It

is shown further that K is not a sensitive function of the distribution function. Thus, enzyme degradation parameters from simple viscometer studies and a knowledge of the power input to the stirred tank are all that are required to estimate enzyme damage in a stirred vessel.

Experimental degradation rates were consistent with the form of equation (3) (i.e., they were proportional to $P^{1/2}$) and were about one-half the predicted rates. This deviation is considered good since Equation 3 contains no adjustable parameters. The degradation rates predicted using various shear distribution functions differed only slightly from each other (< 7%). Although this prevents drawing conclusions on a "preferred" distribution function for stirred tanks, it has the advantage of making the choice of distribution function relatively unimportant to the prediction of enzyme damage.

Finally, equations were derived for the predication of enzyme damage in laminar, tube flow. Two limiting cases were considered: (a) with complete, diffusive radial mixing and (b) with no radial mixing. Again, these limiting cases do not differ greatly from each other and are in agreement with the experimental results of Charm and Wong (Charm, S.E., and B. L. Wong. Enzyme inactivation with shearing. Biotech. and Bioeng. 12:1103, 1970).

To my wife

Sue

ACKNOWLEDGMENTS

TABLE OF CONTENTS

LIST OF TABLES

LIST OF FIGURES

NOMENCLATURE

Symbol	Definition
[A]	concentration of ablumin
a	activity
B	$Z_v \mu L/D$
b	viscometer gap
[C]	catalase concentration
D	diameter
E	activation energy
F	shear distribution function
g	gravitational acceleration
h	height of fluid in stirred tank
K, K', K_i	constant
k, k_o	rate constant
L	Length of tube
m	Reynolds number exponent
n	Froude number exponent
N	frequency of revolution
N_{Fr}	Froude number
N_p	power number
N_{Re}	Reynolds number
P	power
Δp	pressure drop

Symbol	Definition
R_v, R_s, R_t, R_p	rate of enzyme degradation
R	radius, gas constant
r	radial distance
$[S]$, $[S]_0$	substrate concentration
S_v, S_t, S_{vo}, S_p	degradation rate constant
s	shear rate
T	temperature
T_q	torque
t	time
u	linear velocity
V	volume
v	variable volume, voltage
w	weight
x	u/u_{max}
y	axial distance
Z_v, Z_t	degradation parameter
z_{vo}, Z_{to}	frequency factor
μ	viscosity
τ	shear stress
ν	kinematic viscosity
ρ	density

Subscripts	Definition
i	shear distribution model index
lost	activity lost
max	maximum

Subscripts	Definition
min	minimum
o	at $t = 0$
p	pipe
s	due only to shear
t	stirred tank
v	viscometer

I. INTRODUCTION

Enzymes are globular proteins that display catalytic activity. In general, all chemical reactions in a living organism are made possible only through the actions of enzymes (9), yet little is known in molecular terms about how they work. As catalysts they are extremely effective, accelerating reactions 10^8 to 10^{20} times as fast as the uncatalyzed reaction, while being so specific as to distinguish between different substrate isomers. This remakable catalytic activity is achieved by the "active site" and the complex three dimensional structure of the enzyme. The active site is the place of attachment of a substrate molecule and it is surrounded by a three dimensional molecular structure which allows only preferred substrate molecules to fit. The catalytic activity of the molecule depends on the integrity of this active site which is maintained by covalent bonds, hydrogen bonds and van der Waal's forces.

The industrial advantages of enzymes as catalysts are obvious and they are currently being used in many processes, Table 1. However, the fragile nature of proteins and the susceptibility of the active site to chemical and mechanical degradation limits further exploitation of many of the 2000 known enzymes. Enzyme degradation in a shear field has been observed by many investigators (22). Since shear is an ubiquitous component in any industrial or purification process and it is found in many physiological situations, it is an

Table 1. Industrial uses of enzymes (1)

Enzyme	Use
Glucoamylase	Glucose production; saccharification of distillery and brewery mashes; manufacture of fermentation media.
Invertase	Production of confectionaries such as soft-center candies.
Pectic enzymes	Clarification of fruit juices and wines.
Cellulases	Digestive aid; reduction of viscosity of vegetable gums such as those in coffee.
Pancreatin	Digestive aid.
Catalase	Removal of peroxide when it is used for sterilization, especially in milk.
Glucose isomerase	Production of high-fructose corn syrups.
Glucose oxidase	Removal of oxygen from food products; desugars eggs; diagnostic aid (glucose in diabetes).
Microbial protease	Detergent additive; bread baking; chill-proofing beer; meat tenderizer; leather bating.
Bromelain	Digestive aid; anti-inflammatory preparations; meat tenderizer.
Papain	Meat tenderizer; chill-proofing beer.
Rennins	Curdle milk in cheese formation.
Trypsin	Digestive aid; leather bating.
Pepsin	Digestive aid; rennet extender.
α-Amylase	Textile desizing; starch liquefaction; glucose production.
Aminoacylase	Separating DL-acylamino acid into L-amino acid and D-acylamino acid.
Laccase	Drying of laquer.

interesting phenomenon to study.

The object of this work is to examine the potential of a method with which one could measure shear sensitive parameters of an enzyme in a controlled shear situation and then to relate those parameters along with some measurable properties of the process flow system to predict the activity loss of the enzyme in that system.

The procedure used requires that the rate of activity loss as a function of shear stress and temperature be determined. A Couette viscometer was designed for this purpose, consisting of two coaxial cylinders. One is held stationary while the other is rotated at a known rate. A fluid placed in the gap between the cylinders experiences a constant shear rate.

With this relationship and a knowledge of the shear distribution in the process flow system, the rate of activity loss in the system could, in theory, be predicted. A baffled stirred tank was used to generate a shear field with an unknown shear distribution, and various hypothetical forms of this distribution were examined. This type of process vessel is common in many industrial enzyme processes. In addition, laminar flow of an enzyme solution in a pipe is examined by considering two models: (a) assuming complete radial mixing of the enzyme; (b) assuming no radial mixing.

The enzyme catalase was chosen for this study because it can readily be assayed and it has previously been shown (4) to be extremely sensitive to shear.

II. BACKGROUND

Enzymes

The complex molecular structure of enzymes is necessary for catalysis. Globular proteins, of which enzymes are a class, can have as many as four levels of structure. The primary structure refers to the specific amino acid sequence along the covalent backbone of a polypeptide. The secondary structure refers to regular recurring arrangements of the polypeptide chain, such as the helical structure often formed by proteins. The tertiary structure refers to the bent and folded three dimensional shape. The quaternary structure refers to the arrangement of chains to form the unit molecule.

The tertiary and quaternary structures of globular proteins fold compactly and allow very little space for solvent molecules. The internal space of the molecule contains nearly all the hydrophobic groups of the amino acid monomers which further discourages the entry of water, while the external space of a globular protein contains nearly all the hydrophilic amino acid monomers which increases the solubility of the protein in water. The enzyme catalase possesses all four levels of structure.

Catalase catalyzes the decomposition of hydrogen peroxide to oxygen and water. The use of hydrogen peroxide as a substrate as well as a hydrogen acceptor differentiates catalase from peroxidases

4

which require a separate acceptor. Catalase activity is present in nearly all animal cells and in aerobic bacteria. Beef liver catalase has a molecular weight of 240,000 and consists of four subunits each with a molecular weight of 60,000. The catalase molecule has four trivalent iron heme groups which comprise the active group. Under optimum conditions, a single catalase molecule can decompose 5.6 million hydrogen peroxide molecules per minute (12). Catalase is used commercially to remove hydrogen peroxide used in pasteurizing milk prior to cheese making.

Enzyme Degradation

There is a significant amount of literature dealing with shear effects on immobilized enzymes but very little information is available on the effect of shear on free enzymes in solution. The pioneer investigation which examined free enzymes in solution in a controlled shear field was performed by Charm and Wong (4). The enzymes rennet, catalase and carbozypeptidase were studied in a viscometer and some measurements of activity loss of catalase in a teflon tube were reported. The authors reported activity losses of approximately 50% after 90 minutes of shear at 1155 sec^{-1} for all three enzymes. This extreme sensitivity of enzymatic activity to shear led to the conception of this work. The original publication was followed by several others by Charm and co-workers (5,6) in which different types of flow systems were examined and enzyme activity loss was predicted based on the results of the original work. One particular result worth noting because of its' applicability to this work is a 61% loss in catalase activity in a stirred tank after 4 hours of mixing at 1200 RPM.

An exhaustive study of shear degradation of urease in a controlled shear field has been reported by Tirrell (19,20,23) who concluded that urease is permanently inactivated in a shear field only when certain conditions exist; (a) the enzyme must have formed high molecular weight aggregates, and (b) moieties which destroy the sulfhydryl group of cysteine residues are present (20). The oxidation of these sulfhydryl groups was concluded to be catalyzed by iron ions and promoted by shear.

Additional studies conducted by Tirrel (20,21) demonstrated urease and lactic dehydrogenase inactivation to be a function of shear stress rather than shear rate as modeled by Charm. Shear stress is the force per area the adjacent fluid exerts on an enzyme molecule and is therefore a more logical parameter to study than shear rate if molecular deformation is the mechanism of enzyme inactivation. Shear stress is used in this work to model the effect of shear on enzyme activity loss.

III. EXPERIMENTAL APPARATUS

Viscometer

An apparatus was constructed to shear enzyme solutions at con-
trolled shear rates. A Couette viscometer was chosen as the best de-
sign to shear a large volume of a low viscosity fluid. This design
consists of two coaxial cylinders with the fluid to be sheared placed
in the annular space between the cylinders, Figure 1. In this work,
the outer cylinder was rotated at a fixed rate while the inner cylin-
der was held stationary. This method allows stable laminar flow at
higher Reynolds numbers than can be achieved by rotating the inner
cylinder (18).

If the gap between the cylinders is small compared to the di-
ameter, the shear rate experienced by a fluid in laminar flow in the
gap is

$$s = u/b \qquad\qquad (1)$$

where u is the linear velocity of the outer cylinder and b is the gap
between the cylinders. The bottom of the fluid cavity was designed
as a cone and plate viscometer to insure the same shear rate through-
out the fluid.

Since the fluid in the viscometer must be in laminar flow for
Equation 1 to be valid, experiments were performed to determine the
maximum velocity at which the outer cylinder could be rotated without

7
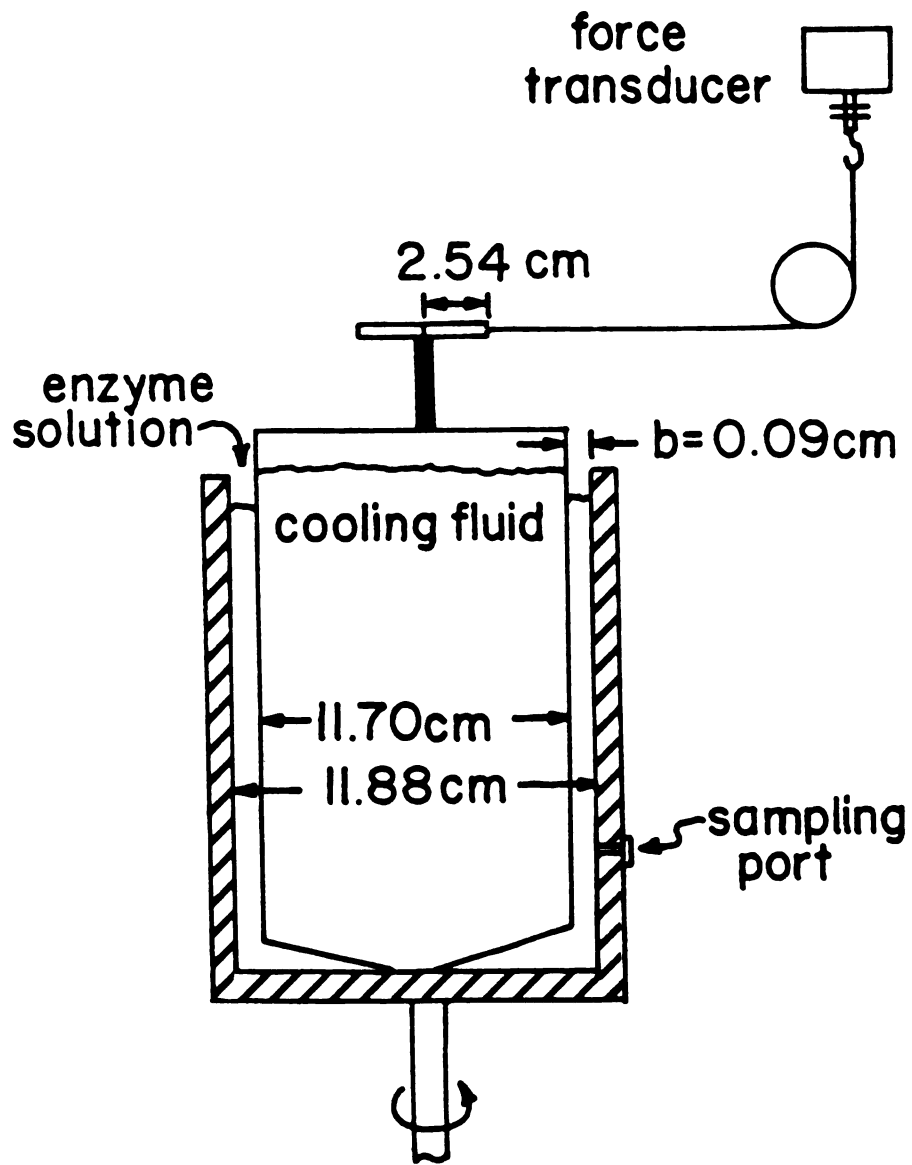
Figure 1. Couette viscometer schematic.

turbulence. This velocity in turn gives the maximum shear rate attainable in the viscometer. The torque transmitted to the fluid and in turn to the inner cylinder was measured by a force transducer as shown in Figure 1. Equation 2 gives the torque for laminar flow (18).

$$T_q = 2\pi^2 \mu h N \frac{D_2^2 D_1^2}{D_2^2 - D_1^2} \tag{2}$$

where μ is the viscosity of the fluid, h is the wetted height of the cylinders, N is the frequency of revolution of the outer cylinder, and D_1 and D_2 are the diameters of the inner and outer cylinders, respectively.

Equation 2 and the experimental data of torque vs. frequency of revolution are plotted on Figure 2 such that one should get a straight line for laminar flow. The velocity at which the measured torque deviates from the predicted straight line indicates the point at which flow becomes instable (i.e., laminar flow and constant shear rate can no longer be maintained) (18). The experimental points measured with the viscometer followed the theoretical line up to a velocity of 155 cm/sec. Thus for water, used in this work, the maximum shear rate attainable in the viscometer is 1700 sec^{-1}.

Since a fluid in a shear field generates heat by viscous friction, the inner cylinder of the viscometer was filled with water at the control temperature to act as a heat sink. Computation of the maximum theoretical temperature rise, assuming the outer cylinder was perfectly insulated and the inner cylinder was at the control temperature, gave an increase which was less than 0.01°C. The fluid
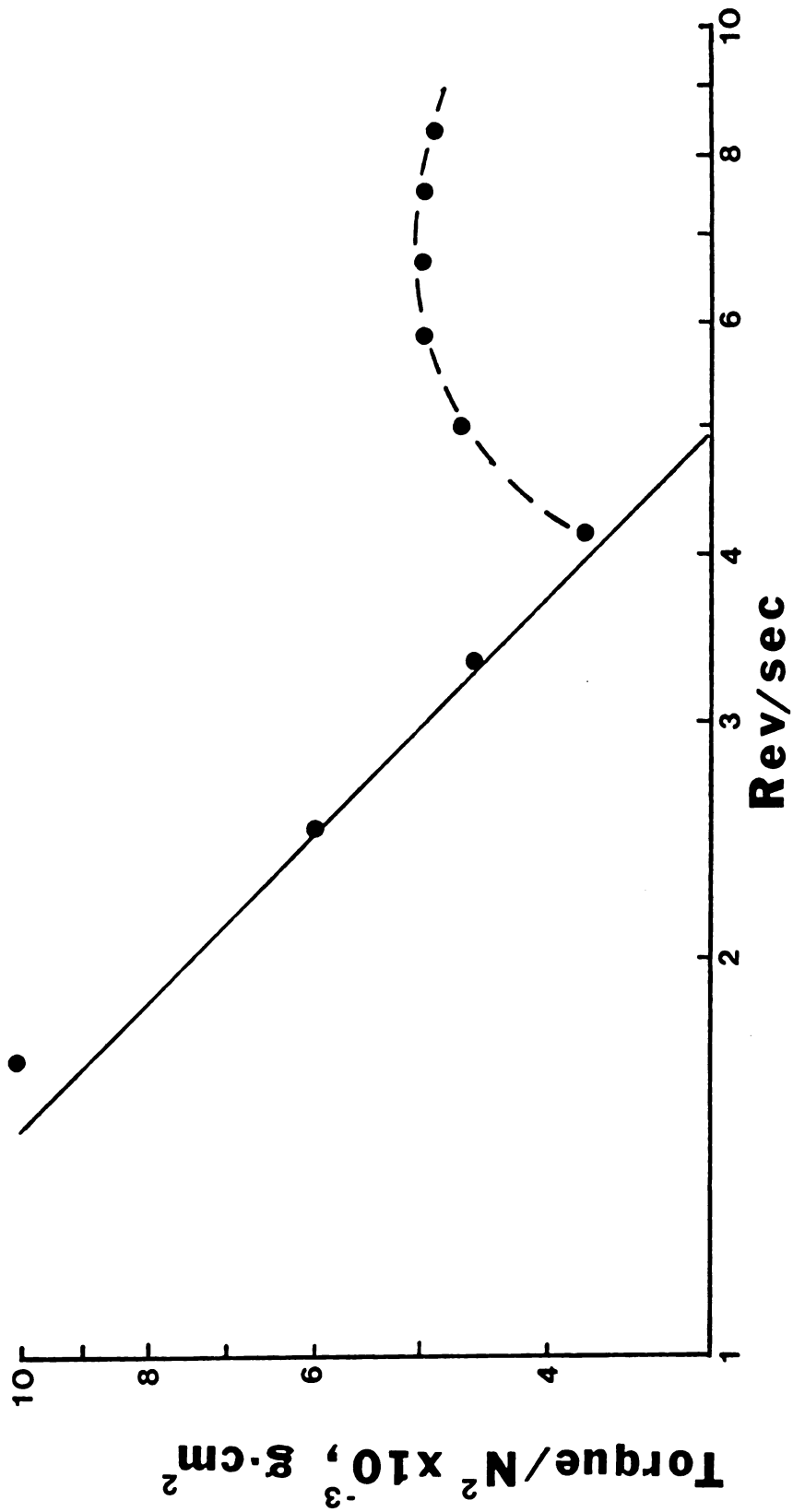
Figure 2. Viscometer torque versus rev/sec. The straight line represents laminar flow, deviation from this line represents transition to turbulence.

temperature measured after several experimental runs was identical to the control temperature within the accuracy of the thermometer (< 0.1°C).

Stirred Tank

A schematic of the stirred tank and dynamometer used in this work are shown in Figure 3. The tank was designed to be geometrically similar to vessels commonly found in industry. The industry standard of four baffles, one twelfth the width of the tank diameter and a radial discharging six-blade turbine impeller was used. The other geometric relationships were based on the following Standard Tank Configurations (8): (a) a fluid depth equal to the tank diameter; (b) an impeller diameter equal to one third of the tank diameter; (c) the impeller distance from the bottom of the tank equal to one third of the tank diameter; (d) the impeller blade width equal to one fifth of the impeller diameter; and (e) the impeller blade length equal to one fourth of the impeller diameter. A cover was used to prevent the fluid from being thrown out at high impeller velocities.

The temperature of the enzyme solution was maintained by circulating water at the control temperature through the tank jacket, preventing any increase in temperature by viscous heating. This procedure was not necessary however, when measuring torque because of the short duration of the experiment. Temperature changes never exceeded 1°C in these experiments.

The dynamometer was used to measure impeller torque. The torque transferred to the fluid is in turn transferred to the tank which rests on the dynamometer turntable. The product of the radius of the turntable pulley (1.59 cm) and the force measured on the force transducer is the torque applied to the fluid by the impeller.
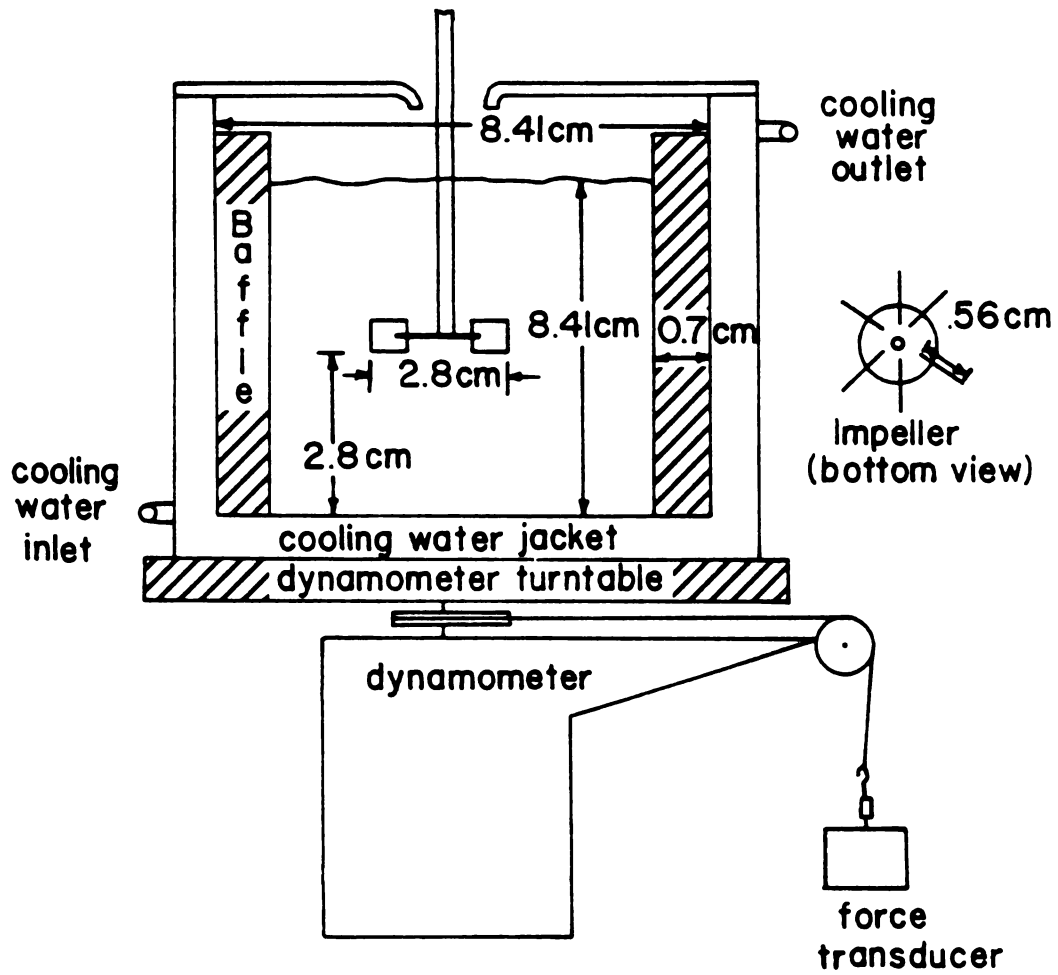
Figure 3. Stirred tank, impeller and dynamometer schematic.

IV. ASSAY METHOD

Bovine liver catalase was purchased from Worthington Biochemical Corporation (code CTS) or Boehringer-Mannheim Biochemicals and was diluted to 5μg/ml with 20 mM potassium phosphate buffer (pH 7.00). Some experiments were performed with the enzyme solution containing 500 μg/ml of bovine serum albumin purchased from Sigma Chemical Company. All experiments were conducted in a constant temperature room.

The enzyme catalyzes the decomposition of hydrogen peroxide to water and oxygen

$$2H_2O_2 \rightarrow 2H_2O + O_2 \tag{2}$$

The reaction as described by Maehly and Chance (13) obeys pseudo first order kinetics.

$$\frac{-d[S]}{dt} = K[C][S] = k[S] \tag{3}$$

where [S] is the concentration of substrate (hydrogen peroxide) and t is time. Since the enzyme concentration [C] is constant throughout the reaction, it may be incorporated in the reaction rate constant k. If $[S]_0$ is the initial concentration of hydrogen peroxide, Equation 3 can be integrated to give

$$\ln [S] / [S]_0 = -kt \tag{4}$$

13

The rate constant is determined by following the concentration of hydrogen peroxide and since k is directly proportional to the activity of the enzyme (13), this parameter is used to monitor degradation.

The concentration of hydrogen peroxide was measured spectrophotometrically by recording the absorbance at 240 nm in a Beckman DK - 2A spectrophotometer. The reference cuvette was filled with 3 ml of 50 mM potassium phosphate buffer (pH 7.00) and a 0.1 ml aliquot of the enzyme solution. The sample cuvette was filled with 3 ml of a solution of 50 mM potassium phosphate buffer (pH 7.00) and 10.5 mM hydrogen peroxide. For an assay, a 0.1 ml aliquot of the enzyme solution was removed from the shearing device with a syringe and injected into the sample cuvette, held at 25°C. Following each assay the sample cuvette was cleaned with a suspension of magnesium oxide in distilled water, rinsed, and then soaked in nitric acid as described by Beers and Sizer (2).

The decomposition of hydrogen peroxide initially obeys first order reaction kinetics but after one minute the rate constant begins to decrease (13). Because the reaction is first order for such a short time it is difficult to assay catalase with precision. For this reason the spectrophotometer was interfaced with a computer.

The output signal from the spectrophotometer was amplified and sent via an analog-to-digital converter, to an IBM 1800 computer, (see Figure 4). The computer was programmed to read these voltage signals 120 times over a period of 0.5 seconds, average them and store this value for each half second interval during the first minute of reaction (the program is listed in Appendix B). The voltage is directly proportional to absorbance read by the spectrophotometer. Since
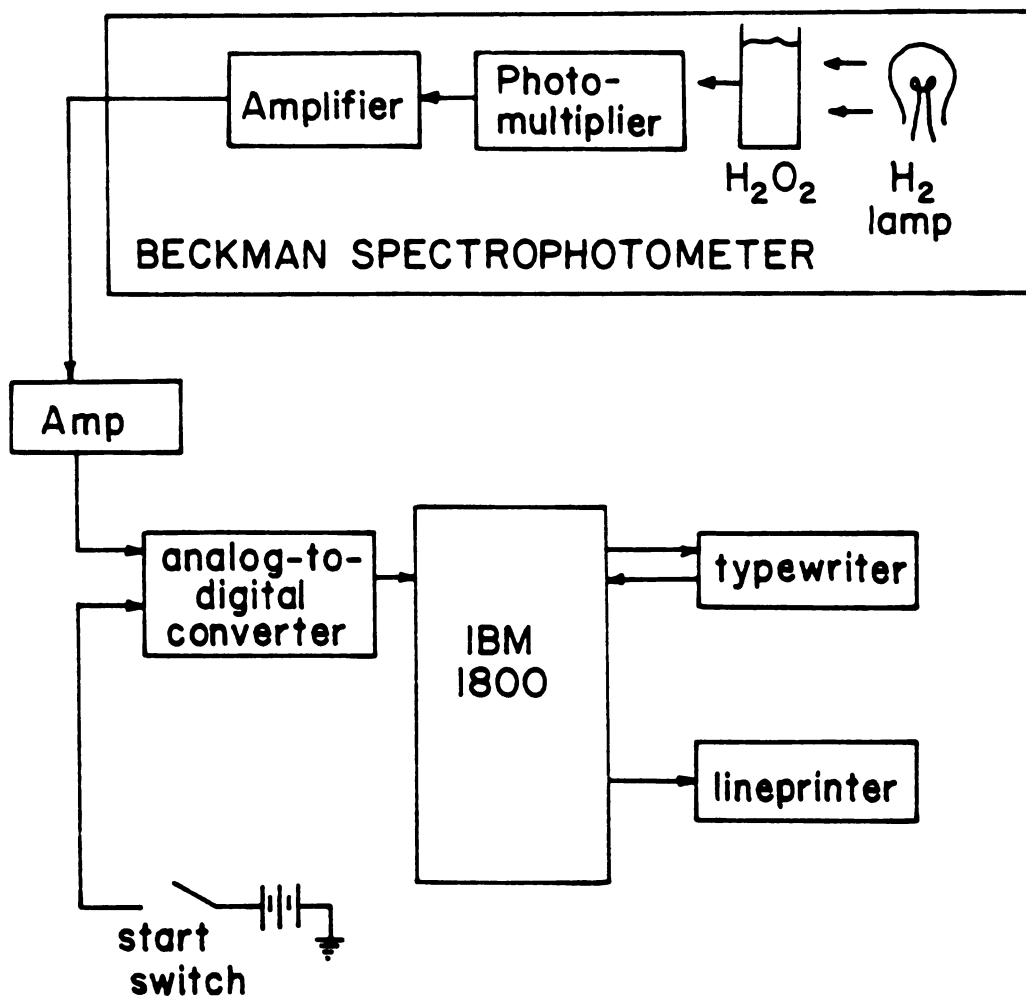
Figure 4. Schematic of the assay apparatus and computer interface.

Beer's law relates concentration to absorbance, the hydrogen peroxide concentration is proportional to the voltage and Equation 4 becomes

$$\ln (v/v_0) = -k\ t \qquad\qquad (5)$$

where v_0 is the voltage at $t = 0$. A linear regression analysis performed by the computer of ln v vs. time yields the rate constant k. The computer was also programmed to plot the results and to analyze the rate constants as a function of shear exposure time.

V. RESULTS AND DISCUSSION

Protein Adsorption to the Viscometer

When a buffered Worthington catalase solution was allowed to remain in the viscometer without the application of shear, the activity of the solution decreased exponentially with time to a steady state level of activity (curves D, E, F, Figure 5). It is speculated that this is due to adsorption of the enzyme on the walls of the viscometer. Enzymes have previously been reported to adsorb to polypropylene test tubes, lucite and glass (7,10,16).

The speculation that the enzyme was adsorbing to the walls of the viscometer is supported by other results: (a) increasing the concentration of catalase decreased the fraction of "adsorbed" enzyme, (curves D and E, Figure 5); (b) increasing the temperature increased the fraction of "adsorbed" enzyme, (curves E and F, Figure 5); (c) the application of shear after the "adsorption" loss reached steady state, increased the activity of the solution (curves D and F, Figure 5). Here, the applied shear stress is assumed to remove some of the enzyme from the viscometer walls. All of this experimental evidence is consistent with a previous report that proteins at a water-solid interface conform to a Langmuir model of adsorption (11).

The addition of albumin to Worthington catalase solutions in the viscometer suppressed the "adsorption" of enzyme (curve C, Figure 5). Presumably, the albumin, which was at a much higher concentration

17
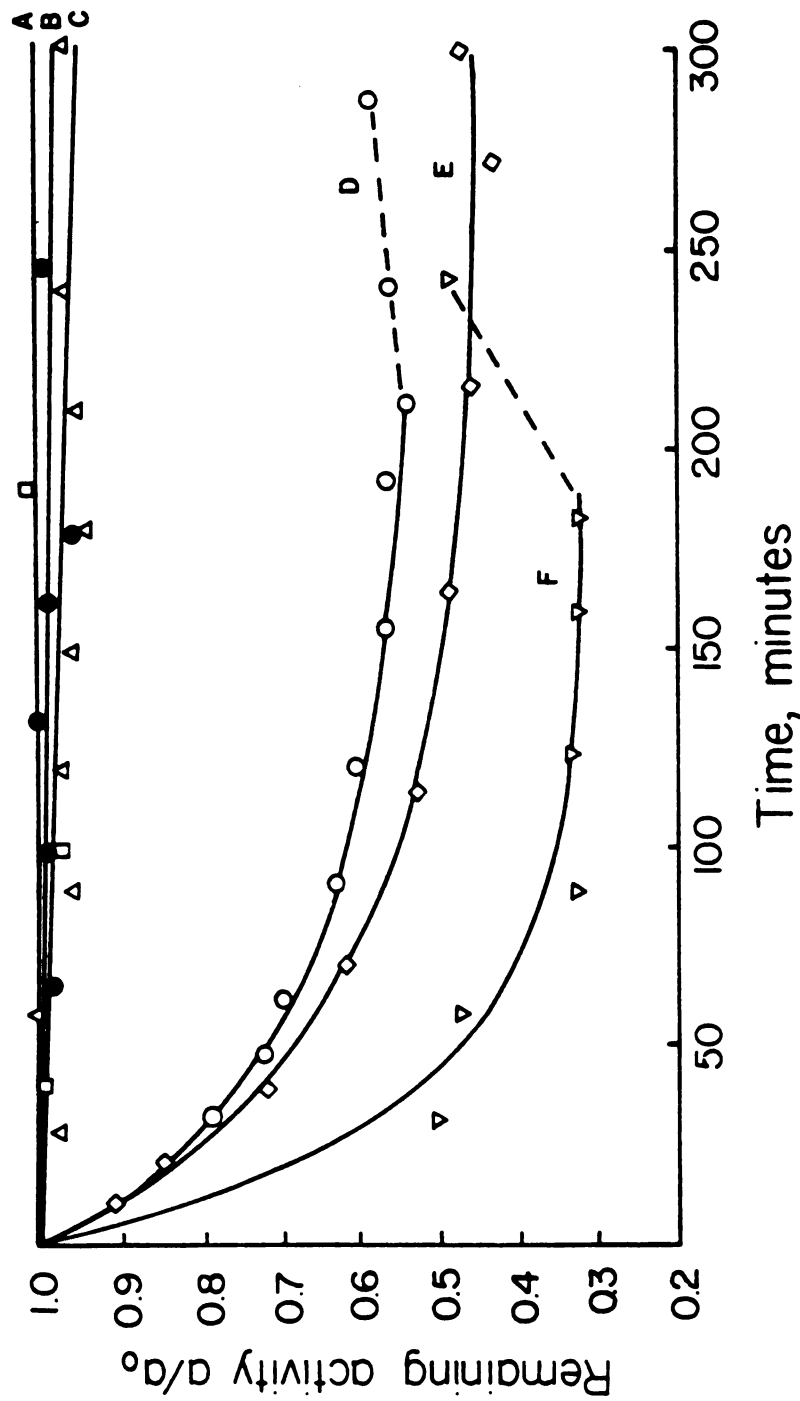
Figure 5. Loss of catalase activity without shear. Dashed lines indicate periods of shear.
(A) □ Boehringer-Mannheim catalase, T = 4°C, [C] = 5 μg/ml, [A] = 0, viscometer;
(B) ● Worthington catalase, T = 20°C, [C] = 5 μg/ml, [A] = 0, stirred tank;
(C) ◁ Worthington catalase, T = 20°C, [C] = 5 μg/ml, [A] = 0.5 mg/ml, viscometer;
(D) ○ Worthington catalase, T = 1°C, [C] = 10 μg/ml, [A] = 0, viscometer;
(E) ◇ Worthington catalase, T = 1°C, [C] = 5 μg/ml, [A] = 0, viscometer;
(F) ▽ Worthington catalase, T = 10°C, [C] = 5 μg/ml, [A] = 0, viscometer.

(500μg/ml) than catalase (5μg/ml), was preferentially adsorbed to the viscometer walls. Albumin was therefore added to all Worthington catalase solutions prepared for viscometer shear experiments.

It was unnecessary to add albumin to catalase solutions in the stirred tank since there was no measurable catalase adsorption in the tank (curve B, Figure 5). This was fortunate since the addition of albumin caused extensive foaming when stirred, which prohibited an assay of the solution. Both the viscometer and the tank were con-structed of stainless steel but the viscometer had a much larger sur-face area to volume ratio and was therefore more susceptible to ad-sorption. Shear experiments carried out with and without albumin in the Couette apparatus indicated that albumin does not affect the shear damage phenomenon.

The Boehringer-Mannheim enzyme did not display the same adsorp-tion phenomenon (curve A, Figure 5). Since the methods of purification used in the preparations are unknown, it is difficult to hypothesize on this discrepancy. However, according to the supplier the Worthing-ton enzyme was sterilized by filtration through a 0.22 μm pore size membrane which may have removed microbiological contaminants that pre-vented adsorption of the Boehringer-Mannheim enzyme.

Catalase Degradation in a Constant Shear Field

Since the rate constant for hydrogen peroxide decomposition, k, is proportional to enzymatic activity, a, a_0 (units of activity/ volume) will be used in lieu of k, k_0 respectively.

Assuming a first order reaction mechanism, the rate of shear deactivation in a batch reactor is given by

$$R_v = \frac{-da}{dt} = S_v \, a \tag{6}$$

where S_v, the rate constant for activity loss, is expected to be a function of the shear field and the sensitivity of the enzyme to shear. The first order assumption (rate of activity loss proportional to remaining activity) is an intuitive model which fits the experimental data reasonably well, Figure 6.

Upon integration, Equation 6 yields

$$a/a_0 = e^{-S_v t} \tag{7}$$

S_v and a_0 can be obtained from measured values of activity as a function of exposure time. Linear regression was used to estimate the values of S_v and a_0. Several experiments were run at different temperatures and shear stresses to determine the effect of these variables on the rate constant S_v.

Shear stress τ for a Newtonian fluid is defined by

$$\tau = \mu s \tag{8}$$

where μ is the viscosity of the fluid and s is the shear rate. By substituting Equation 1 for s in Equation 8, it is apparent that the shear stress applied to the enzyme solution in the viscometer can be controlled by varying the linear velocity u, of the viscometer outer cylinder.

$$\tau = (\mu/b) \, u \tag{9}$$

The viscosities of all enzyme solutions used in this work (including those that contained albumin) were essentially the same as that of
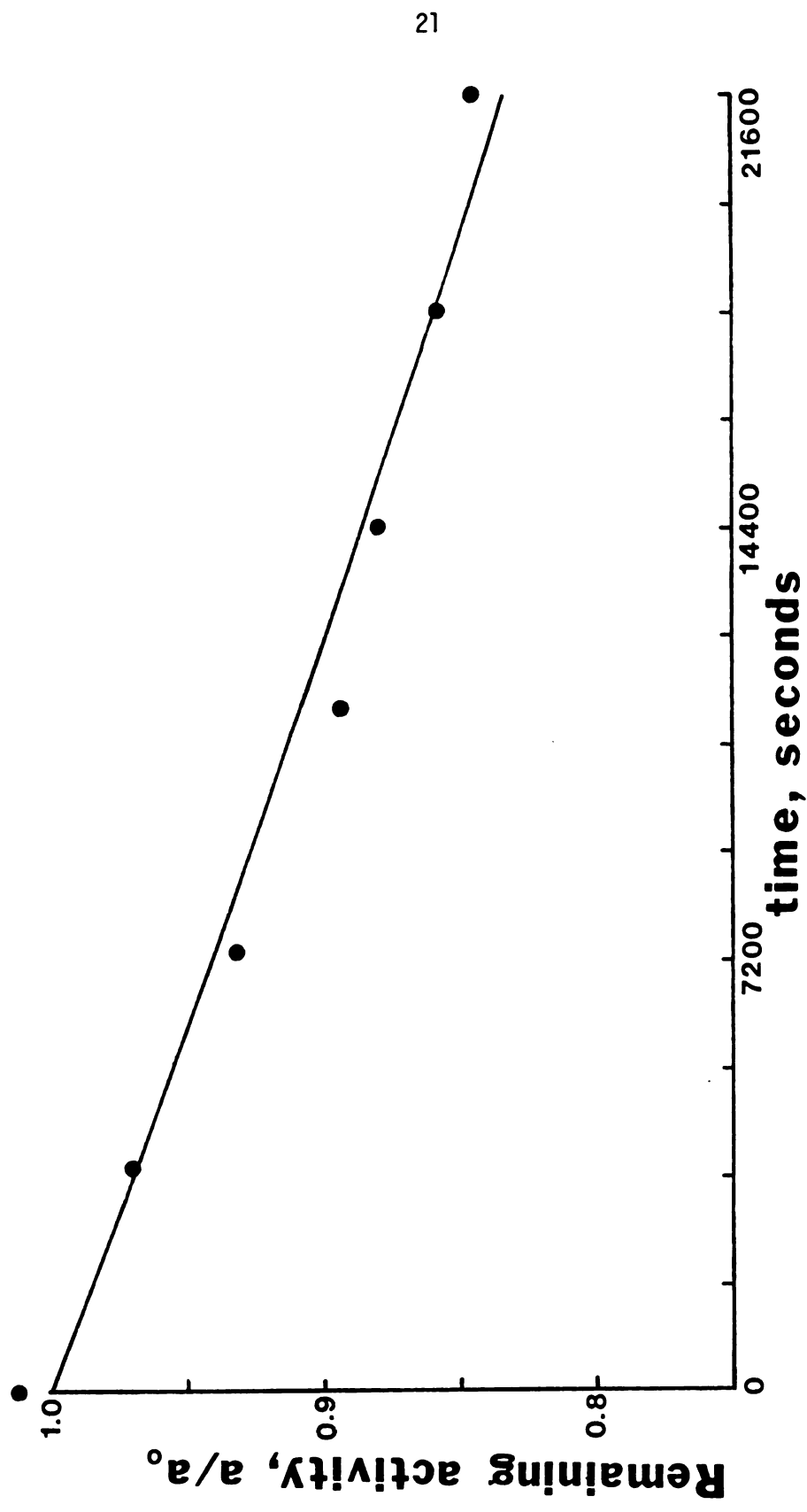
Figure 6. Remaining activity versus exposure time in the viscometer. $\tau = 30.98$ dynes/cm^2, $T = 2°C$, $S_v = 8.393 \times 10^{-6}$ sec^{-1}, $a_0 = 8.717$ sec^{-1}.

water (17).

At each temperature (2°C, 10°C, 20°C) measurements were made at different shear stresses to find the effect on S_v. The degradation rate constant appears to increase linearly with an increase in shear stress (Figure 7), such that one may write:

$$S_v = Z_v\tau + S_{vo} \qquad (10)$$

where Z_v and S_{vo} are the slope and intercept of a plot of S_v versus τ. S_{vo} is the rate constant of activity loss in the viscometer in the absence of shear and is a function of the properties of the viscometer. The rate of loss due only to shear then becomes

$$R_s = S_v a = Z_v(\tau)a = Z_v(\mu s)a \qquad (11)$$

where the subscript s refers to the shear effect only. Equation 11 describes the rate of degradation at shear rate s.

Shear Distribution Function

Definition

It would be useful to be able to predict shear deactivation in a flow process from information about the shear sensitivity of the enzyme (obtained from Couette type data), and information that is related only to the shear field in the process. This type of modeling could in theory be achieved if the distribution of shear throughout the flow system were known.

One can define a shear distribution function in the following way. Let F ds be the fraction of fluid in the vessel which is experiencing a shear rate between s and s + ds. Then the rate of
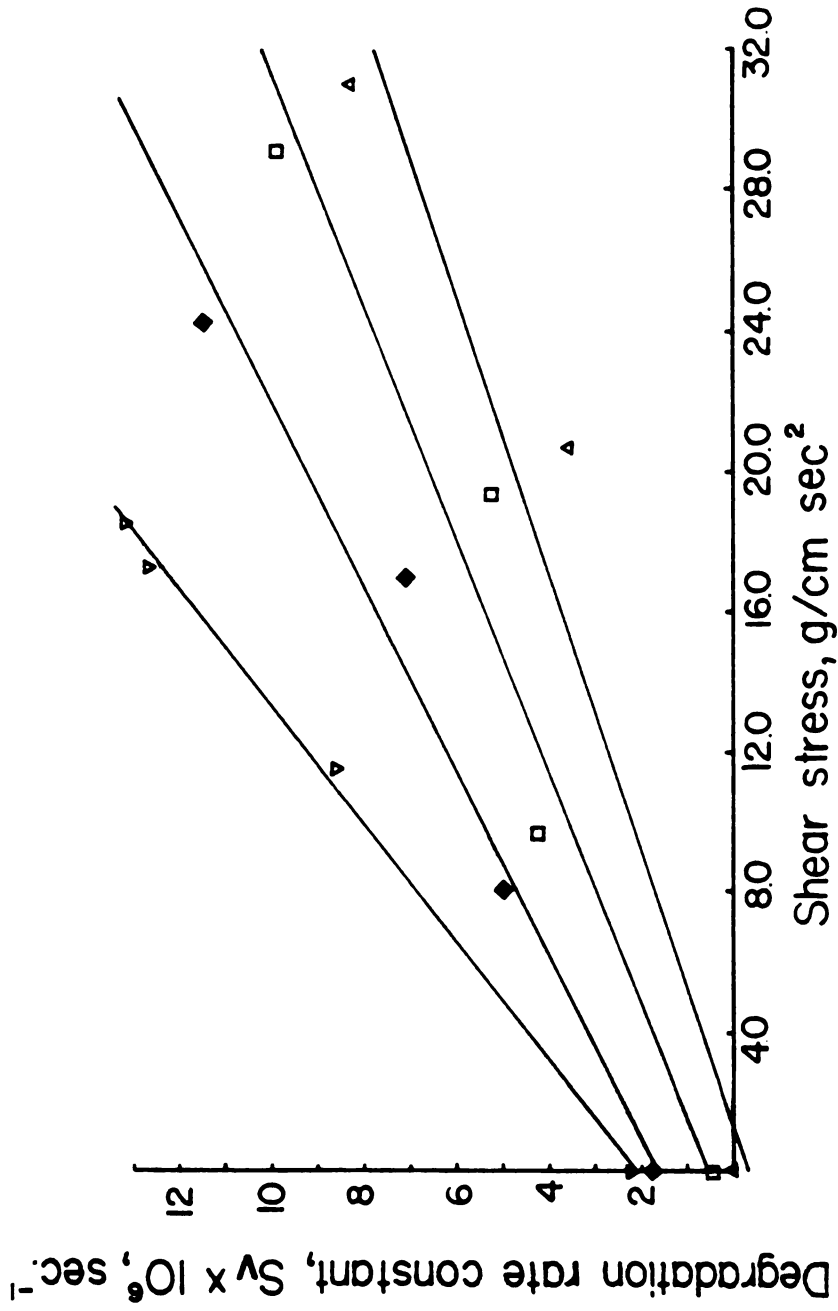
Figure 7. Viscometer degradation rate constants versus shear stress. Worthington catalase with albumin $\triangle$, T = 2°C, Z_v = 2.54 x 10^{-7} cm sec/g, S_o = -3.07 x 10^{-7} sec^{-1}; $\blacklozenge$, T = 10°C, Z_v = 3.81 x 10^{-7} cm sec/g, S_o = 1.66 x 10^{-6} sec^{-1}; $\triangledown$, T = 20°C, Z_v = 5.94 x 10^{-7} cm sec/g, S_o = 2.09 x 10^{-6} sec^{-1}; Boehringer-Mannheim catalase without albumin, $\square$, T = 4°C, Z_v = 3.01 x 10^{-7} cm sec/g, S_o = 5.68 x 10^{-7} sec^{-1}.

degradation of enzyme in this volume element is:

$$R_s \, F \, ds \qquad (12)$$

where R_s is the rate of deactivation of enzyme experiencing a shear rate s (see Equation 11), which can be measured in a viscometer. Then the total rate of deactivation of enzyme in the process vessel is found by integrating Equation 12 over all shear rates
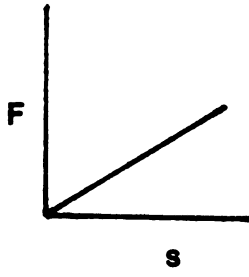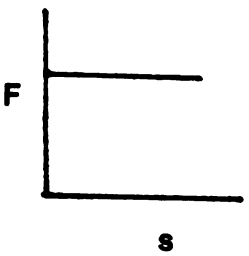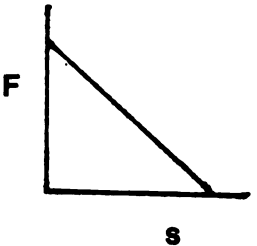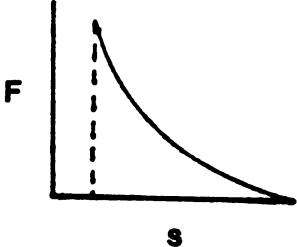
$$R_t = \int_0^\infty R_s \, F \, ds \qquad (13)$$

Thus, if one has data for deactivation as a function of shear (i.e., R_s from viscometer type data) and a shear distribution function F for the process vessel, one should be able to calculate the total rate of degradation in the vessel.

Application to a Stirred Tank

In general F is an unknown function. This difficulty was approached by assuming functions of F and examining the resultant rate expressions. Four models of F were proposed (Table 2): Model 1 assumes that most of the fluid in the tank is being sheared at a high rate; Model 2 assumes that the various shear rates (up to a maximum value) are equally likely; Model 3 assumes that most of the fluid in the tank is under low shear; and Model 4 assumes that shear rate decays exponentially with distance from the center of the tank as reported by Holland and Chapman (8). A comparison of experimental degradation rates with predicted rates from the various models might be expected to give some insight into the actual distribution of shear in the tank.

Table 2. Shear distribution function models.

Model	Plot	F(s)
1		$\dfrac{2}{s_{max}^2}\, s$
2		$\dfrac{1}{s_{max}}$
3		$\dfrac{2\,(s_{max} - s)}{s_{max}^2}$
4		$-2\, \dfrac{\ln(s/s_{max})}{[\ln(s_{min}/s_{max})]^2\, s}$

The method used to derive shear distribution functions can be explained by examining Model 1, in which F increases linearly with S, such that

$$F = Ks \quad \text{for} \quad 0 \leq s \leq s_{max} \tag{14}$$

where s_{max} is the maximum shear rate allowed by this model.

The constant K can be evaluated in terms of s_{max} with the use of the restriction

$$1.0 = \int_0^\infty F \, ds \tag{15}$$

which is apparent from the definition of F. By substituting Equation 14 into 15 and integrating the result, one obtains an expression to replace K in Equation 14, thus

$$F = (2/s_{max}^2)s \tag{16}$$

which is the form of Model 1 shown in Table 2. A similar procedure was used to derive Models 2 and 3.

If Equations 16 and 11 are substituted into Equation 13, the total rate of enzyme degradation R_t in the tank becomes

$$R_t = \int_0^\infty Z_v(\mu s) \, a \, \left\{\frac{2}{s_{max}^2}\right\} \, ds \tag{17}$$

This equation contains the enzyme activity (a) which will be treated as a constant with respect to s. This is valid if one assumes that there exists packets of fluid which are experiencing a shear rate s, and the packets are continuously being destroyed and reformed

(micromixing), such that the activity of the entire volume of fluid is nearly the same at any given instant. This is consistent with the idea of a shear distribution function which assumes that there is always the same distribution of shear but a given molecule is not necessarily confined to a constant shear region. In fact, in many turbulent flow systems there may not be any constant shear regions.

With this assumption Equation 17 can be integrated to give

$$R_t = \frac{2}{3} Z_v \mu s_{max} \ a \tag{18}$$

which expresses the total rate of degradation in the tank as a function of s_{max}.

One method for estimating s_{max} employs the rate of energy dissipation in a fluid with shear rate s, which is given by (3):

$$d\dot{P}/dV = \mu s^2 \tag{19}$$

where P is power, and V is the volume of the tank. It is assumed that Equation 19 is valid for all of the fluid with shear rate s, so that the total rate of energy dissipation is given by

$$P = \int_0^s \mu V_s^2 \ F ds \tag{20}$$

If Equation 16 is used to replace F in Equation 20 and the resulting expression is integrated over all allowable shear rates, one obtains an expression for s_{max},

$$s_{max} = (\frac{2P}{V\mu})^{1/2} \tag{21}$$

This equation can be substituted in Equation 18 to yield

$$R_t = K_i \ Z_v \ (\frac{\mu P}{V})^{1/2} \ a = -\frac{da}{dt} = S_t \ a \tag{22}$$

where the index i refers to a particular distribution model (e.g., $K_1 = 0.943$). The other models produced a similar result, differing only in the value of K_i, see Table 3.

Integration of Equation 22 gives a theoretical relationship describing the remaining catalase activity as a function of exposure time in the stirred tank

$$a/a_0 = e^{-S_t t} \qquad (23)$$

The measured activity of catalase after exposure to shear in the tank is plotted in Figure 8 and appears to be consistent with the assumed first order rate of degradation. Experimental values of the degradation rate constant S_t, obtained from such data are listed in Table 3.

The derivation of Model 4 required a different approach because it has a more fundamental origin. Model 4 may be written

$$s = s_{max} e^{-kr} \qquad (24)$$

where r is the radial distance away from the center of the tank, and k is constant. F ds (the volume fraction of fluid which is experiencing a shear rate between s and s+ds) when equated to a differential volume element is

$$Fds = \frac{dv}{V} \qquad (25)$$

where dv is the differential volume and V is the total volume of the system. The shear distribution function can now be expressed

$$F = \frac{1}{V}(-\frac{dv}{ds}) = \frac{1}{V}\frac{dv}{dr}(-\frac{dr}{ds}) \qquad (26)$$

where the "chain rule" has been utilized to separate dv/ds into two

Table 3. Shear distribution function results.

$$S_t = K_i Z_v (\mu P/V)^{1/2}$$

N = 3000 RPM

Model	K_i	$S_t \times 10^3$ min^{-1}	
		T = 10°C	T = 20°C
1	0.943	1.07	1.44
2	0.866	0.98	1.33
3	0.816	0.92	1.25
4*	0.986	1.11	1.51
experimental	-	2.21	2.82

*$s_{min}/s_{max} = 0.5$
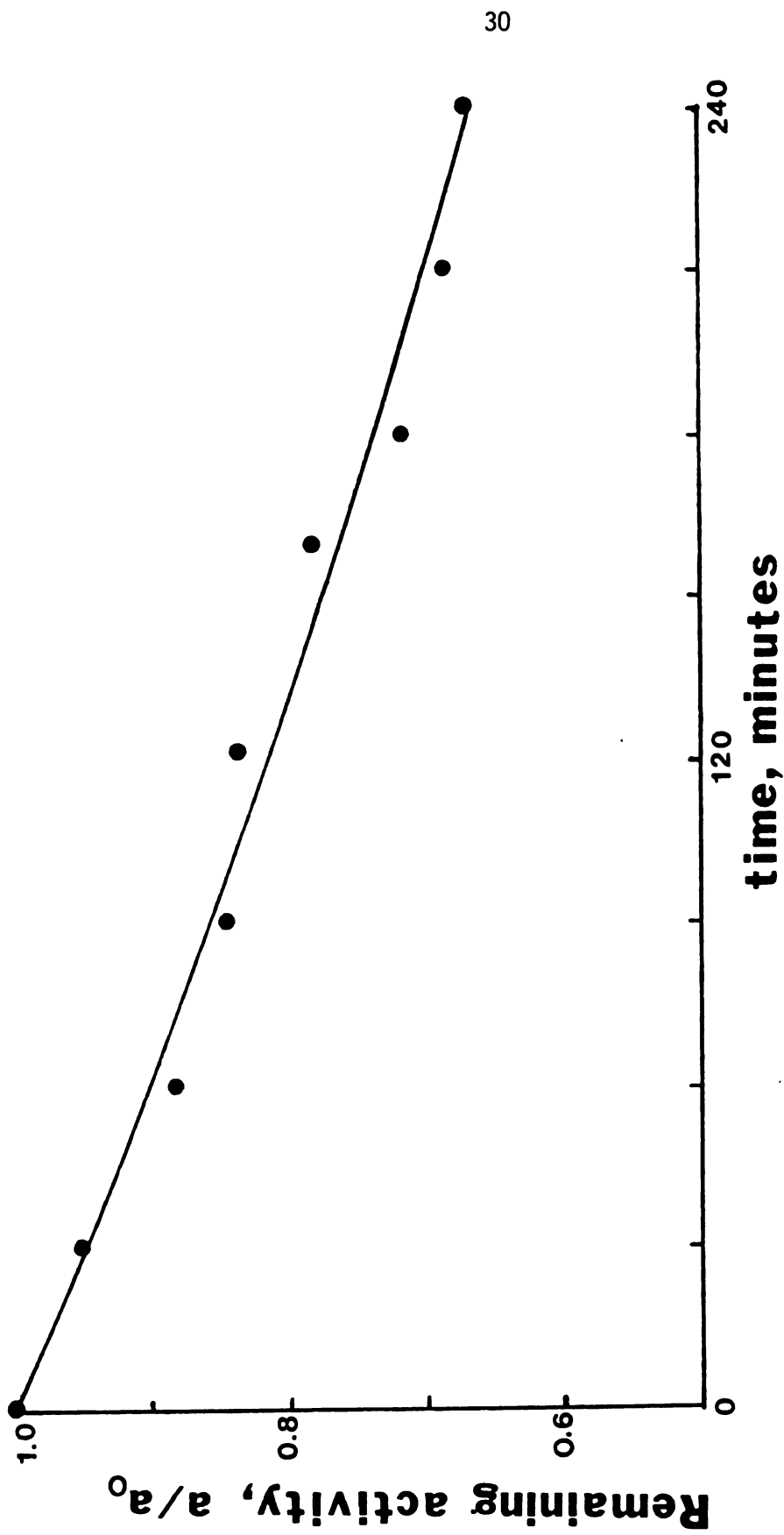
Figure 8. Remaining activity versus exposure time in the stirred tank. N = 2000 RPM, T = 20°C, S_t = 16.93 x 10-4 min-1, a_0 = 8.13 sec-1.

easily acquired derivatives. The derivative of r with respect to s (from Equation 24) is

$$-\frac{dr}{ds} = \frac{1}{ks} \tag{27}$$

The change in volume fraction of the tank with respect to r is

$$\frac{1}{V}\frac{dv}{dr} = \frac{2\pi hr}{V} \tag{28}$$

where h is the height of the fluid in the tank. By substituting Equations 27 and 28 into 26 one obtains

$$F = \frac{2\pi hr}{Vks} \tag{29}$$

When Equation 24 is substituted for r in Equation 29 the shear distribution function becomes

$$F = \frac{-2\pi h}{Vk^2}\frac{\ln(s/s_{max})}{s} \tag{30}$$

which is a function of the variables s and the unspecified constants k and s_{max}. Equation 24 can be rearranged to express k as a function of s_{min} (the minimum shear rate which the fluid experiences at the wall of the tank).

$$k = \frac{-\ln(s_{min}/s_{max})}{R} \tag{31}$$

Substitution of Equation 31 into 30 yields the form of Model 4 which is shown in Table 2.

$$F = \frac{-2}{[\ln(s_{min}/s_{max})]^2}\frac{\ln(s/s_{max})}{s} \tag{32}$$

Unlike the other models examined, Model 4 is a two parameter model (s_{min}, s_{max}), therefore the elimination of S_{max} with Equation 20 yields

a value of K_4 which is a function of s_{min}.

The maximum value of K_4 is obtained when s_{min} equals s_{max}, which is tantamount to a process which has a single shear rate, such that Equation 19 becomes

$$s = (\frac{P}{V\mu})^{1/2} \tag{33}$$

One can, therefore express the rate of degradation directly from Equation 11 as

$$R_t = Z_v \ a \ (\frac{\mu P}{V})^{1/2} \tag{34}$$

which implies that K_4 equals one.

The deactivation rates predicted by the various models (as a function of $P^{1/2}$) and the experimental degradation rate constants measured in the stirred tank are shown in Figure 9. Because of the small differences in the predicted rates, it is difficult to choose the better model, however this is advantageous since it implies that the predicted rate is insensitive to the form of the shear distribution function. The agreement between the predicted rates and the experimental rates is acceptable when one considers that Equation 22 contains no adjustable parameters, and the viscometer experimental error inherent in measuring such small deviations from the initial activity. The attractive aspect of this result is that the form of the prediction is consistent with the data (i.e., degradation rate is proportional to $P^{1/2}$).
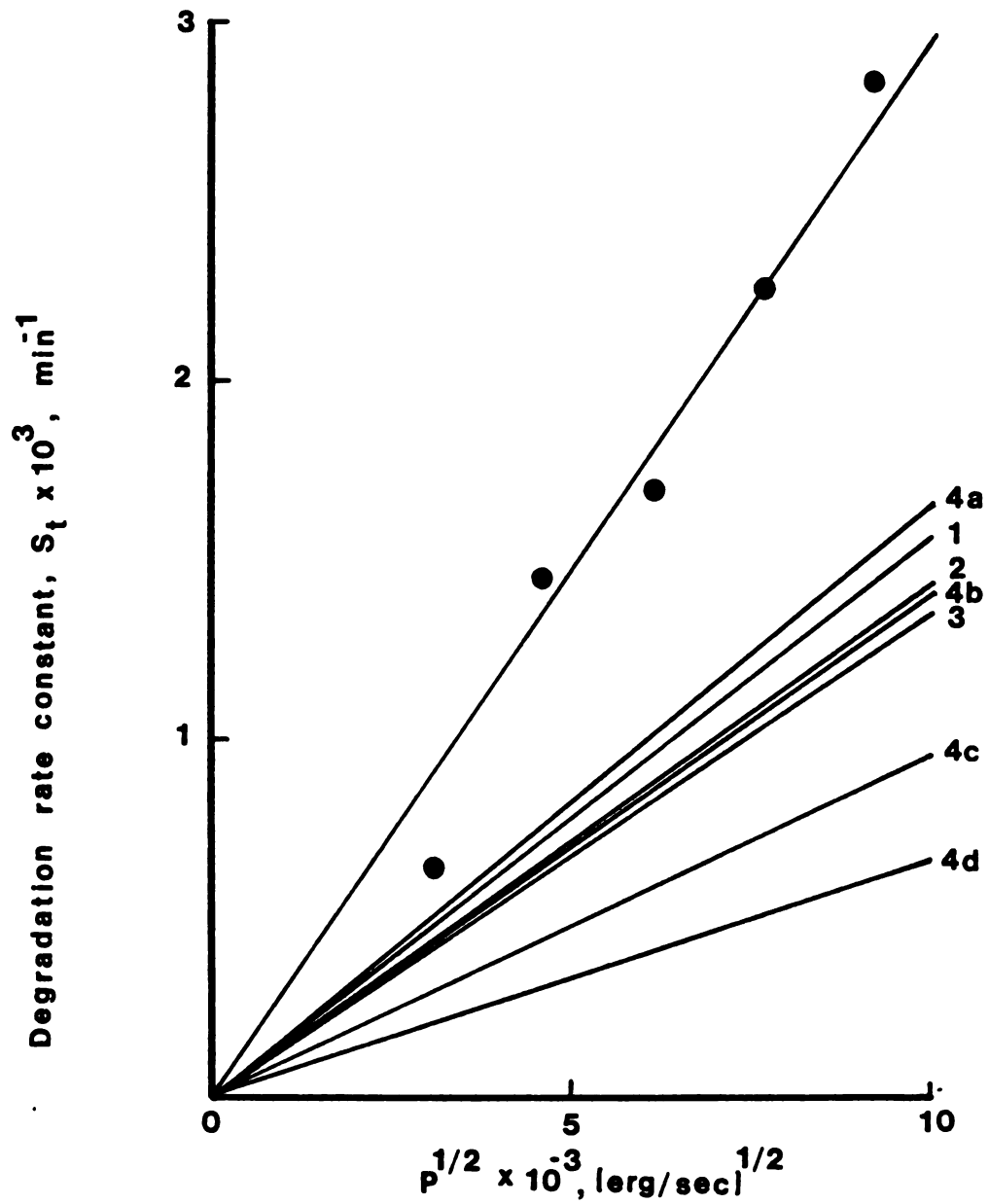
Figure 9. Stirred tank degradation rate constants versus $P^{1/2}$.
● Experimental points. Numbers refer to shear distribution models. T = 20°C.
4a, s_{min}/s_{max} = 1.000; 4b, s_{min}/s_{max} = 0.100;
4c, s_{min}/s_{max} = 0.010; 4d, s_{min}/s_{max} = 0.001.

Stirred Tank Power Measurement

The use of Equation 21 to predict the rate of enzyme degradation requires knowledge of the power requirements of the tank. The dimensionless equation for agitator power in a stirred tank is given by (15):

$$N_p = K \ (N_{Re})^m \ (N_{Fr})^n \tag{35}$$

where N_p is the power number, N_{Re} is the Reynolds number and N_{Fr} is the Froude number. These dimensionless numbers are defined by the equivalent equation:

$$\frac{P}{N^3 D^5 \rho} = K \ (\frac{D^2 N}{\nu})^m (\frac{N^2 D}{g})^n \tag{35a}$$

where:

P = power

N = frequency of revolution

D = impeller diameter

ν = kinematic viscosity

ρ = density

g = gravitational acceleration

K, m, n = empirical parameters.

In general, at high Reynolds numbers ($\geq 10^4$) m is equal to zero, and if the tank is baffled n is equal to zero, therefore the power number is constant and power is proportional to N^3 (8).

For stirred tanks, power is related to torque by

$$P = T_q \ (2\pi N) \tag{36}$$

where the quantity in parenthesis is the rate of angular displacement.

Dynamometer measurements of torque were used to calculate power in the stirred tank at various values of N and ν, Figure 10. Although this tank was baffled, the power number is constant with respect to Reynolds number only for constant Froude numbers, which is similar to the results obtained by Rushton et al. (15) in unbaffled tanks.

The Froude number represents a ratio of inertial to gravitational forces and affects the shape of the liquid surface (24). Large waves were observed near the baffles, and since maintainance of a vortex in an unbaffled tank is responsible for a Froude number dependence (24), it is presumed that these waves produced a similar result in this tank. This effect would be minimized in a larger tank where the waves would be dissipated over the larger surface area.

Because of the Froude number effect, torque was found to be linear with the frequency of revolution N (see Figure 11) such that one may write:

$$T_q = K' N \tag{37}$$

where K' is constant. If Equations 36 and 37 are substituted into Equation 22 one obtains

$$S_t = K_i Z_v \left(\frac{2\pi K'}{V}\right)^{1/2} \mu^{1/2} N = Z_T \mu^{1/2} N \tag{38}$$

Equation 38 suggests that the degradation rate constant is proportional to $\mu^{1/2} N$ which can be seen in a plot of experimental data measured at various temperatures, Figure 12. The intercepts on Figure 12 could not be distinguished from zero for an 80% confidence interval (14).

A similar result would be expected in a stirred tank operating
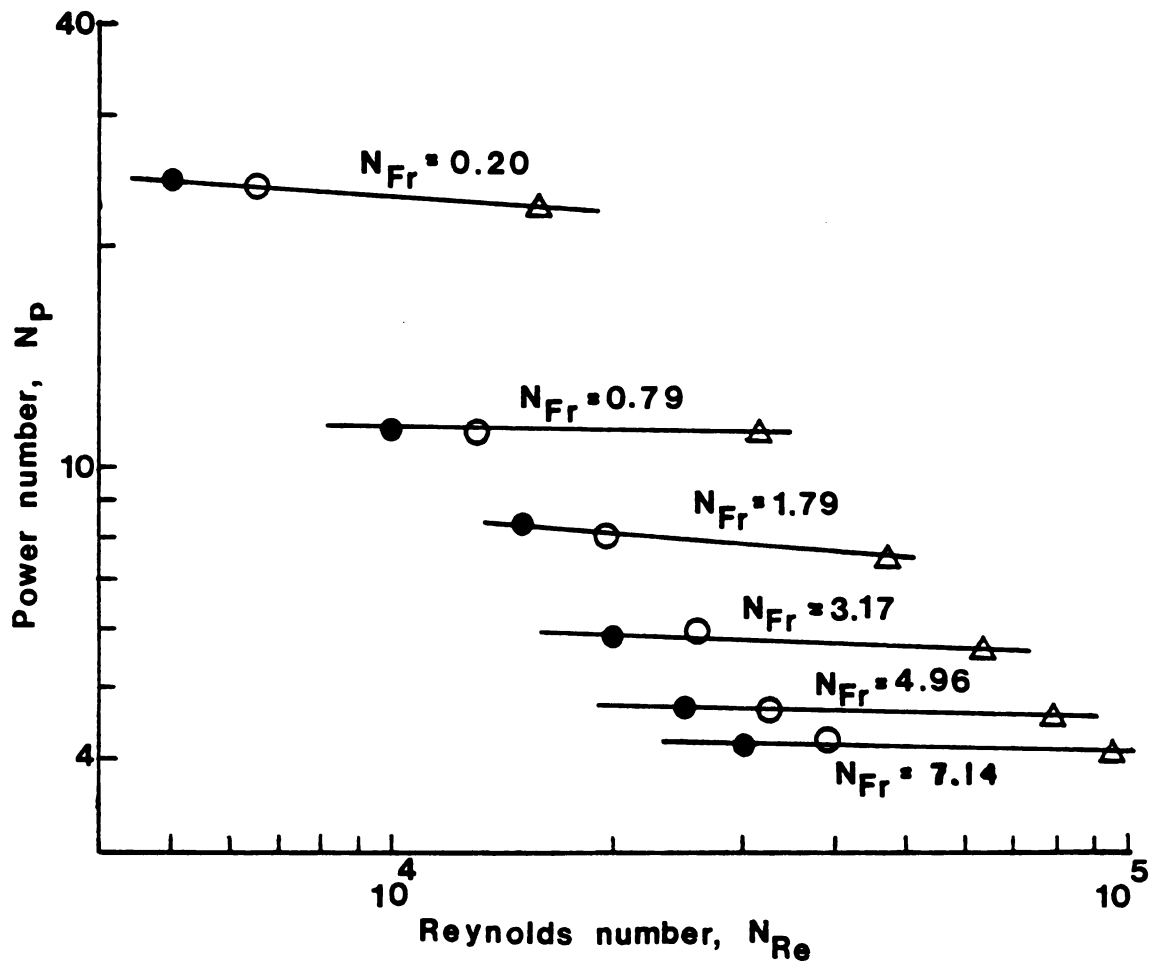
Figure 10. Power curve for stirred tank.

ν = 0.01307 cm^2/sec ●
ν = 0.01002 cm^2/sec ○
ν = 0.00326 cm^2/sec △
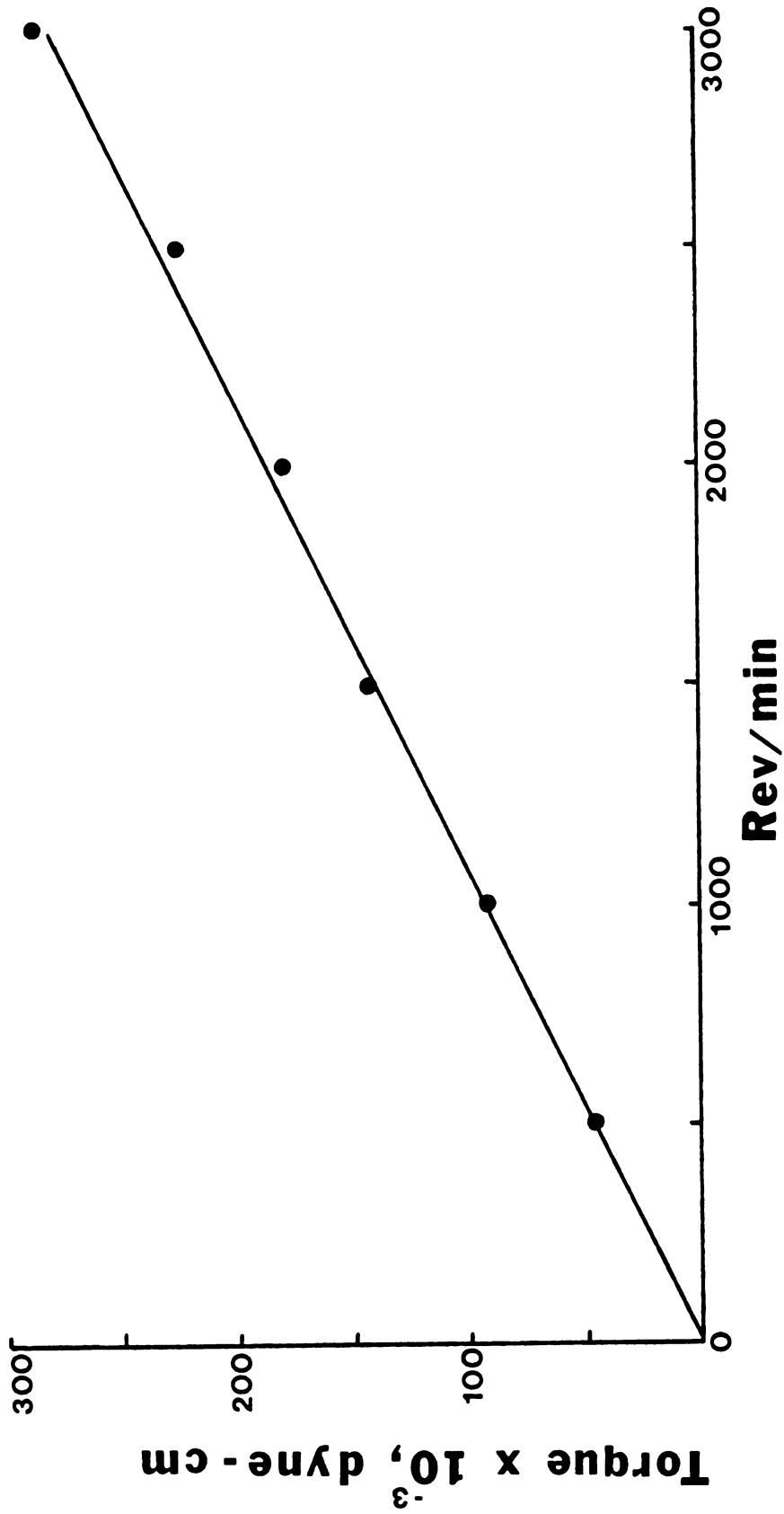
Figure 11. Dynamometer measured torque versus RPM, $\nu = 0.01307$ cm^2/sec.
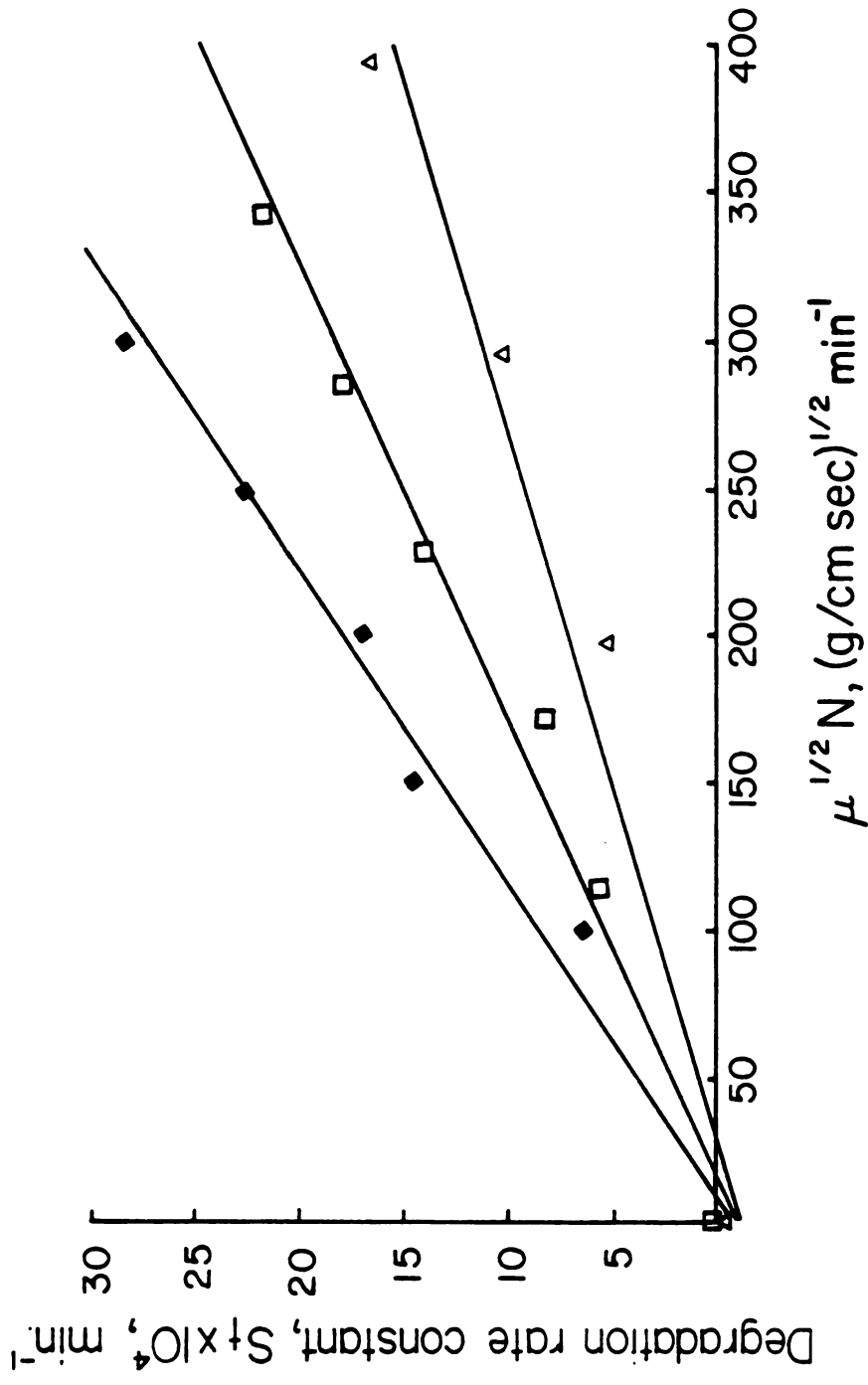
Figure 12. Stirred tank degradation rate constants versus $\mu^{1/2} N$. $\triangle$, $T = 1°C$, $Z_t = 4.16 \times 10^{-6}$ min^{-1}, $\square$, $T = 10°C$, $Z_t = 6.45 \times 10^{-6}$ min^{-1}, $\blacklozenge$, $T = 20°C$, $Z_t = 9.38 \times 10^{-6}$ min^{-1}.

Y-axis: Degradation rate constant, $S_t \times 10^4$, min^{-1}

X-axis: $\mu^{1/2} N$, (g/cm sec)$^{1/2}$ min^{-1}

in the viscous region where Equation 37 would also be valid. In general however, with a baffled stirred tank in the turbulent range, the degradation rate should be proportional to $(\mu N^3)^{1/2}$ but this has not been demonstrated here.

Activation Energy of Degradation

Increasing temperature accelerated the rate of deactivation in the viscometer (Figure 7). If one assumes the rate of enzyme degradation in a shear field follows classical reaction kinetics, temperature dependence of the rate (Equation 11), can be described by an Arrhenius relationship:

$$Z_v = z_{vo}e^{-E/RT} \tag{39}$$

where the parameter z_{vo} and E are the frequency factor and activation energy respectively, and R is the gas constant (1.987 cal/g mole °K). Values of Z_v obtained from Figure 7 for various temperatures were fit to Equation 39, see Figure 13. Equation 11 now becomes

$$R_s = z_{vo}\tau e^{-E/RT} a \tag{40}$$

The frequency factor z_{vo} and the activation energy E obtained from a least squares fit of the data were 0.262 cm sec/g and 7564 cal/g mole respectively.

Equation 40 implies that catalase molecules must acquire a critical energy E from the shear field before they will degrade. The Boltzmann factor $e^{-E/RT}$ therefore, is the fraction of molecules that have attained this energy, and the product $z_{vo}\tau$ is the rate at which this fraction degrades.
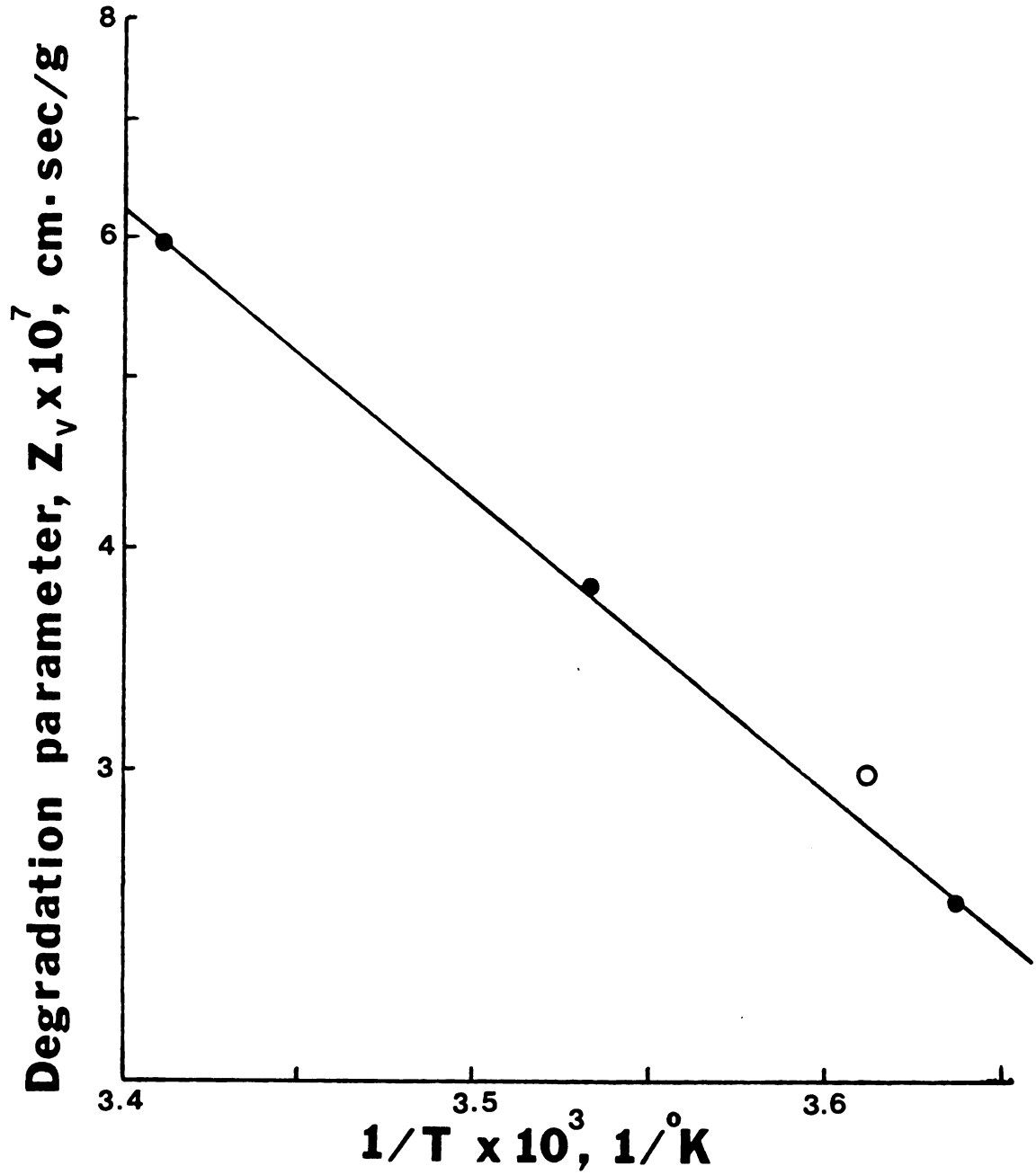
Figure 13. Viscometer degradation parameter, Z_v versus T^{-1}. E = 7564 cal/gmole. ● Worthington catalase; ○ Boehringer-Mannheim catalase.

Experiments using the Boehringer-Mannheim catalase (without albumin) were also carried out and the resultant values of S_v and Z_v are shown in Figures 7 and 13. These results were not used to calculate the Arrhenius parameters of Worthington catalase (with albumin), but were included to show that they are consistent.

As observed in the viscometer the rate of activity loss in the stirred tank increased with temperature, Figure 12. If shear induced catalase degradation is an activated process, then the activation energy should be the same in any flow system. The Arrhenius relationship for the stirred tank (Equation 38) is

$$Z_t = z_{to}e^{-E/RT} \tag{41}$$

Experimental values of Z_t versus T^{-1} are shown in Figure 14. The activation energy from the stirred tank was 6825 cal/g mole, which is consistent with the value of 7564 cal/g mole obtained from viscometer data. This excellent agreement in activation energy in two greatly different flow systems supports the theory that enzyme degradation is an activated process and that the activation energy is quite small.
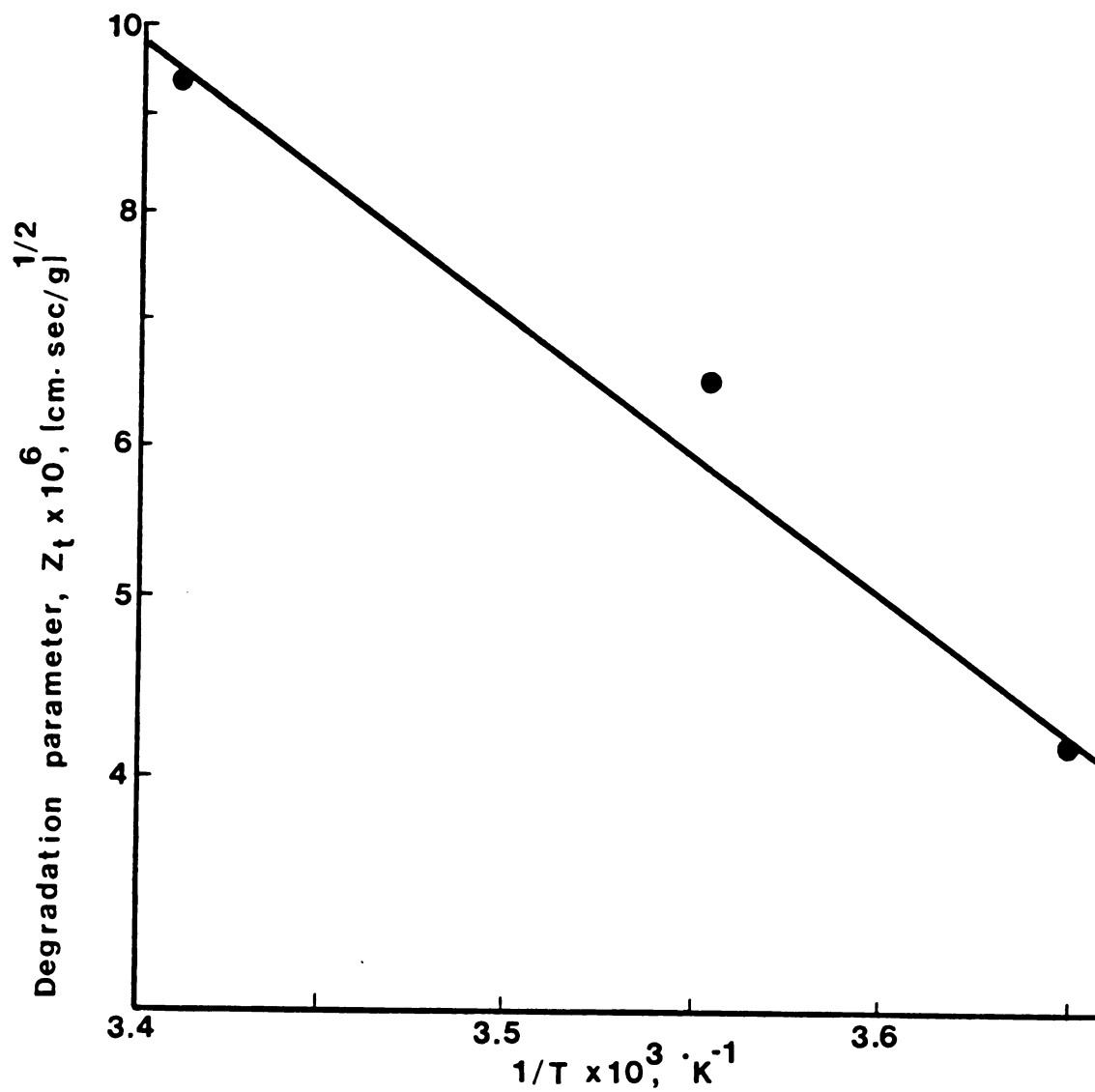
Figure 14. Stirred tank degradation parameter, Z_t versus T^{-1}.
E = 6825 cal/gmole.

VI. DEGRADATION IN POISEULLE FLOW

Laminar fluid flow in a pipe (Poiseulle flow) exhibits a radial velocity profile which is maximum at the center of the pipe and decreases parabolically to zero at the wall. The analysis of Poiseulle flow of an enzyme solution through a pipe is an interesting problem because it possesses characteristics of both the viscometer and the stirred tank. There is a distribution of shear in the pipe as in the stirred tank, but at any radial position the shear rate is constant as in the viscometer. In the analysis of the stirred tank it was assumed that the fluid was well mixed and the activity throughout the fluid was constant which allowed the integration of Equation 17. In laminar pipe flow however, a fluid particle remains in its' lamina as it travels down the length of the pipe and mixing occurs primarily through molecular diffusion. This situation was examined by developing two limiting cases: (a) assuming the fluid is radially well mixed, and (b) assuming no radial diffusion. These results are compared to the experimental data of Charm and Wong (5).

Pipe Flow with Complete Radial Mixing

If radial mixing is assumed, the shear distribution function can be used to estimate the rate of deactivation in the pipe. This function can be derived with the use of Equation 26. Shear rate in Poiseulle flow is given by

$$s = -\Delta pr/2\mu L \tag{42}$$

where r is the radial distance from the center and Δp is the pressure drop along the length L of the pipe (3). The derivative of r with respect to s is then:

$$-\frac{dr}{ds} = \frac{2\mu L}{\Delta P} \tag{43}$$

The derivative of v with respect to r is given by Equation 28 and the product becomes

$$F = \frac{4\mu L^2 \pi r}{V \Delta p} = \frac{16\mu L r}{D^2 \Delta p} \tag{44}$$

where D is the diameter of the pipe. Substitution of r with Equation 42 gives the shear distribution function for the pipe.

$$F = 32 \ \{\frac{\mu L}{D \Delta p}\}^2 \ s \tag{45}$$

If Equations 11 and 45 are used with Equation 13 the folowing integral is obtained:

$$R_p = \int_0^{s_{max}} Z_v \ (\mu s) \ a \ 32 \ (\frac{\mu L}{D \Delta p})^2 \ s \ ds \tag{46}$$

This is analagous to Equation 17 derived for the stirred tank and as previously discussed the activity will be treated as a constant in the radial direction. An expression for s_{max} can be obtained from Equation 42 by substituting the pipe radius for r. The integration of Equation 46 yields:

$$R_p = \frac{\Delta p \ D \ Z_v \ \mu \ a}{6 \ L} \tag{47}$$

which is the total rate of activity loss in the pipe. Since this

model assumes complete radial mixing, the shear exposure time is the
residence time in the pipe which is given by (3):

$$t = \frac{\pi R^2 y}{Q} \qquad (48)$$

where R is the radius, Q is the volumetric flow rate and y is the
axial distance. Thus the rate of degradation in the pipe can be ex-
pressed in terms of pipe length with the use of Equation 48.

$$R_p = \frac{-da}{dt} = \frac{-Q}{\pi_R 2} \frac{da}{dy} = \frac{\Delta p \, D^2}{32 \, L} \frac{da}{dy} \qquad (49)$$

Substitution of Equation 47 into 49 and integrating the result yields
an expression for the remaining activity in the fluid leaving the tube

$$a/a_0 = e^{\frac{-16}{3} B} \qquad (50)$$

$$B = Z_v \, \mu \, L/D \qquad (51)$$

where B has been defined for later reference. Equation 50 is a model
predicting the remaining activity expected after an enzyme solution
has passed through a pipe of length L and diameter D in laminar flow,
assuming complete radial mixing (curve B, Figure 15). This is the
same result obtained by Charm and Wong (5) using a different approach.

Pipe Flow Without Radial Mixing

Since the activity of enzyme varies radially in this model, the
shear distribution method (i.e., Equation 13) is not appropriate. A
different method is used in which the degradation rate in a differential
element of fluid (2πrdrdy), with constant activity, is integrated over
the length of pipe L, then over radius to give the total rate of deg-
radation in the tube. The ratio of total rate of degradation to the

$$B = Z_V \mu L/D$$
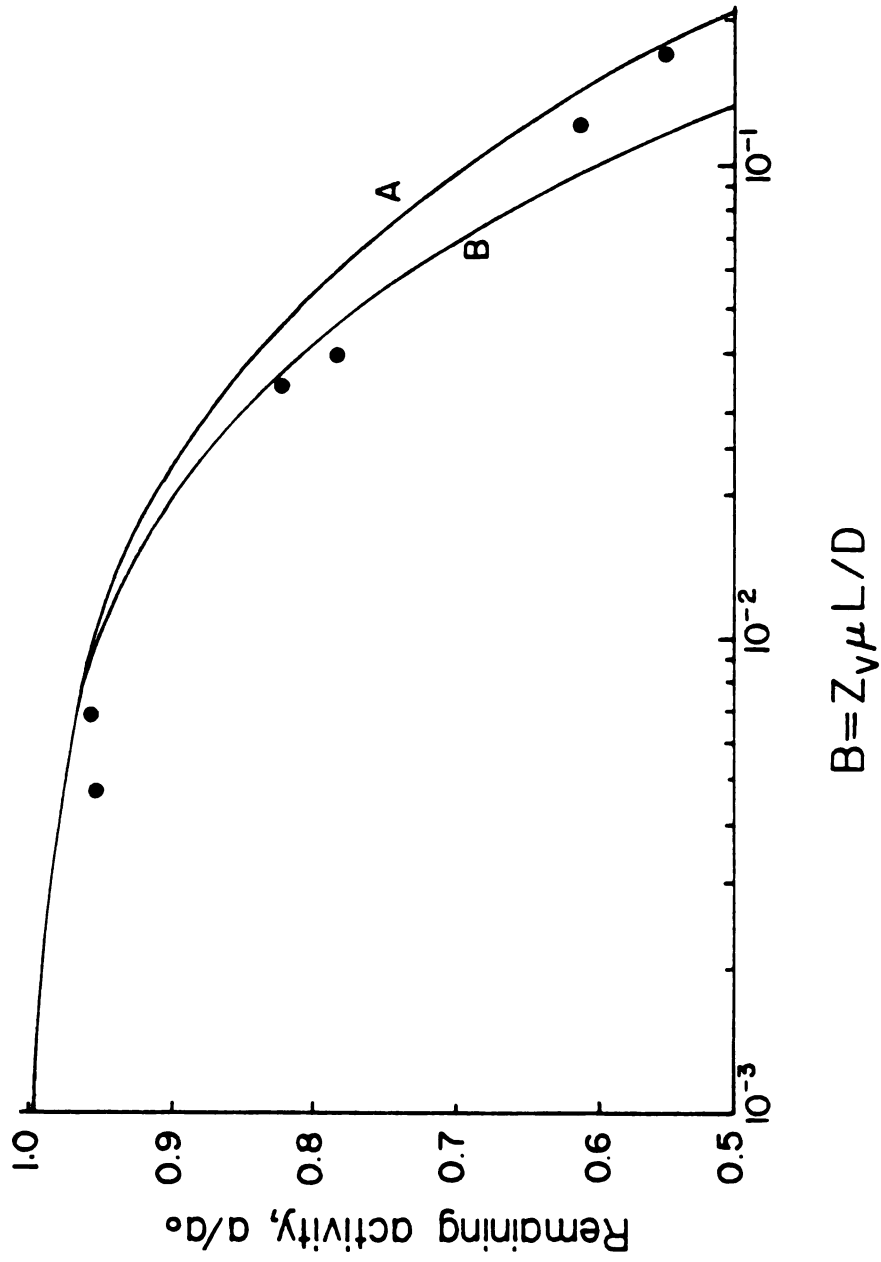
Figure 15.   Remaining activity after laminar flow through a tube. Curve A assumes no radial mixing. Curve B assumes complete radial mixing. The experimental points are from Charm and Wong (4).

rate of active enzyme entering the tube is the total fraction of
activity lost in the flow system.

The degradation rate in the element of fluid (activity/time) is
the product of the shear degradation rate R_s (activity/volume time) and
the volume as follows

$$(R_s)dv = (Z_v \mu sa) \, 2\pi r dy dr \tag{52}$$

Before this equation can be integrated, the variables (a) and (s) must
be related to (y) and (r).

The activity (a) can be expressed as a function of s and t by
combining Equations 7 and 11 as follows

$$a = a_0 e^{-K_v \mu s t} \tag{53}$$

The time (t) that a particle of fluid has been in the pipe (and under
shear) is

$$t = y/u \tag{54}$$

where the velocity u is a function of r. The ratio of velocity to
maximum velocity in Poiseulle flow is given by (3)

$$u/u_{max} = 1 - (r/R)^2 = x \tag{55}$$

where the variable x has been defined to facilitate the derivation.
The maximum velocity is

$$u_{max} = \frac{\Delta p R^2}{4 \mu L} \tag{56}$$

By combining Equations 42 and 56 shear rate can be expressed as

$$s = 2u_{max} \, r/R^2 \qquad (57)$$

If Equations 54 and 57 are substituted into Equation 53 and the variables r and u eliminated with the use of Equation 55 the activity as a function of position is

$$a = a_0 \, e^{-Z_v\mu 4y(1-x)^{1/2}/x} \, dx \qquad (58)$$

The derivative of r with respect to x is found from Equation 55

$$\frac{dr}{dx} = \frac{-R}{2\sqrt{1-x}} \qquad (59)$$

Substitution of Equations 55, 57, 58 and 59 into Equation 52 yields an expression for the total rate of degradation in the pipe.

$$R_p = -Z_v\mu a_0 \pi D u_{max} \int_1^0 \int_0^L \sqrt{1-x} \, e^{\frac{-4B\sqrt{1-x}\,y}{x}} \, dy \, dx \qquad (60)$$

where B is defined by Equation 51. The rate of active enzyme entering the tube is

$$a_0 Q = \frac{a_0 \pi \Delta p R^4}{8\mu L} = \frac{u_{max}\pi D^2 a_0}{8} \qquad (61)$$

where Q is the volumetric flow rate through the pipe. Integration of Equation 60 and division by 61 gives an expression for the total fraction of activity lost.

$$(a/a_0)_{lost} = 2 \int_1^0 xe^{-4B\sqrt{1-x}\,/\,x} \, dx + 1 \qquad (62)$$

The fraction of remaining activity is calculated by substracting Equation 62 from one, which yields

$$a/a_0 = 2 \int_0^1 xe^{-4 \sqrt{1-x} / x} \, dx \qquad (63)$$

Equation 63 describes a model predicting the remaining activity expected after an enzyme solution has passed through a pipe of length L and diameter D in laminar flow, assuming no radial mixing (curve A, Figure 15).

These two models predict nearly the same degradation for B less than 10^{-2}, however for larger values of B the non-mixing model predicts a progressively greater amount of remaining activity than the mixing model. This is because in the non-mixing model, the enzyme in the low shear core of the pipe will remain there, while in the mixing model, all of the enzyme is continuously cycled through the high shear region near the wall. Experimental degradation data would be expected to fall between the predictions of the models.

Experimental catalase degradation data from shear in a viscometer measured by Charm and Wong (5) were fit to Equation 11 to obtain Z_v. This parameter was used to calculate values of B corresponding to experimental degradation data from shear in a teflon tube, also measured by Charm and Wong (5), Figure 15. These data are consistent with the models.

Neither of the models predicts that the total degradation rate is a function of velocity of the enzyme solution. The effect of increased shear rates at higher velocities is exactly compensated by lower exposure times.

VII.   CONCLUSIONS

The goal of this work was to outline a procedure to predict
the activity loss of an enzyme solution in complicated flow systems
of practical interest (e.g., a stirred tank). The procedure consists
of two parts: (a) obtaining the rate of activity loss as a function
of shear stress using a viscometer; (b) this relationship is coupled
with a function describing the distribution of shear (F) to predict
the total enzyme degradation rate in the tank. The final expression
has the form:

$$R_t = K_i Z_v \ (P\mu/V)^{1/2} \ a \qquad (64)$$

where K_i depends on the form of the shear distribution function. Thus,
Z_v obtained from viscometer measurements and P from power measurements
are the only variables which are required to estimate the degradation
rate in a stirred tank with the proposed method.

Enzyme degradation is modeled as a first order kinetic expres-
sion because intuitively one expects the rate of degradation to be a
function of the concentration of active enzyme present. The rate con-
stant from viscometer measurements appeared to be linear with shear
stress. This assumption led to a prediction that the degradation rate
in the stirred tank was proportional to $P^{1/2}$, which was found to be
consistent with experimental evidence. Furthermore, this relationship
is independent of Reynolds number or the type of flow in the tank.

The degradation rates predicted by Equation 64 were about half of the experimental rates. This deviation is probably due to the experimental error in measuring activity loss in the viscometer, where the loss was rarely more than 10%, compared to the activity loss in the stirred tank, where as much as 50% was lost. Significant experimental error may also be expected from the small values of power measured with the dynamometer. A viscometer which was capable of higher shear rates should lessen this error and a larger stirred tank would have a greater power requirement.

The differences between the stirred tank degradation rates predicted by the four shear distribution models were not sufficient to allow conclusions to be made on the form of a "preferred" model. This circumstance however, strengthens the proposed method because the predicted degradation rate is relatively insensitive to inaccuracies in the shear distribution function. For example: if one assumes the minimum shear rate in Model 4 was 50% of the maximum, the predicted degradation rate increases from 0.96 to 1.64×10^{-3} min^{-1}. Therefore, if the deviation between theoretical and experimental rate is primarily experimental error in viscometer data as proposed, even an inelegant shear distribution model should be expected to yield acceptable results with adequate viscometer data.

Another potential method of estimating the rate of enzyme degradation in a stirred tank is dimensional analysis. Experiments could be conducted in a small stirred tank and the results used for larger tanks, by scaling up with the square root of power as suggested by Equation 64. This would eliminate the need for viscometer experiments and the concomitant problems of adsorption and insufficient

shear rates.

The degradation activation energy measured in two kinds of apparatus (the viscometer and the stirred tank) are in reasonable agreement and are approximately 7.0 kcal/g mole. This is near that which would be expected in breaking at most, two hydrogen bonds. The disruption of such bonds may allow a conformational change which reduces the activity of the molecule.

A surprising result of this study is the lack of agreement with Charm and coworkers (4), even though the experimental conditions seem identical. Charm observed 45% of catalase activity remaining in the viscometer after 90 minutes of shear at 1155 sec^{-1}. This may be compared to Figure 6 in which 85% of catalase activity remained after 360 minutes at 1854 sec^{-1}. Since it is difficult to imagine a mechanism by which an enzyme molecule is protected from shear, and in view of the fragile chemical nature of enzymes, it would seem that Charm's observed catalase degradation was at least partly caused by something other than shear. The deactivation of urease in a shear field is enhanced by Fe^{+3} and protein aggregation (22). It is possible that Charm's catalase solutions contained similar contaminants which induced excessive deactivation. It should be noted however, that Charm's viscometer data are consistent with his experiments for flow in a tube (see Figure 15 and references 4,5,6). Thus, it appears that his data and the data from this work are both internally consistant but are not in agreement with each other.

BIBLIOGRAPHY

BIBLIOGRAPHY

1. Bailey, J. E., and D. F. Ollis. Biochemical engineering fundamentals. McGraw-Hill, New York 1977.

2. Beers, R. F. and I. W. Sizer. A spectrophotometric method for measuring the breakdown of hydrogen peroxide by catalase. J. of Biol. Chem. 195:133, 1952.

3. Bird, R. B., W. E. Stewart and E. W. Lightfoot. Transport phenomena. Wiley, New York, 1960.

4. Charm, S. E., and B. L. Wong. Enzyme inactivation with shearing. Biotech. and Bioeng. 12:1103, 1970.

5. Charm, S. E., and C. J. Lai. Comparison of ultrafiltration systems for concentration of biologicals. Biotech. and Bioeng. 13:185, 1971.

6. Charm, S. E., and B. L. Wong. Shear inactivation in mixing biological material. Biotech. and Bioeng. 20:451, 1978.

7. Felgner, P. L. and J. E. Wilson. Hexokinase binding to polypropylene test tubes. Anal. Biochem. 74:631, 1976.

8. Holland, F. A. and F. S. Chapman. Liquid mixing and processing in stirred tanks. Reinhold, New York, 1966.

9. Karlson, P. Introduction to modern biochemistry. Academic Press, New York, 1968.

10. Kobamoto, N., G. Lofroth, P. Camp, G. Van Amburg, L. Augenstein. Specificity of trypsin adsorption onto cellulose, glass, and quartz. Biochem. and Biophys. Res. Comm. 24:622, 1966.

11. Laylin, J. K., and Augenstein. Adsorption of enzymes at interfaces: Film formation and effect on activity. Adv. in Enzym. 28:1, 1966.

12. Lehninger, A. L. Biochemistry: The molecular basis of cell structure and function. 2nd Ed., Worth, New York, 1975.

13. Maehly, A. C., and B. Chance. The assay of catalase and peroxidases. Meth. of Biochem. Anal. Interscience Publishers, New York, 1:357, 1954.

14. Neter, J., and W. Wasserman. Applied linear statistical models. Irwin, Illinois. 1974.

15. Rushton, J. H., E. W. Costich, and H. J. Everett. Power charteristics of mixing impellers. Chem. Eng. Prog. 46:385, 1950.

16. Smith, C. L. The inactivation of monomolecular films of protein and it's relations to the lifetime of active radicals formed in water by X-radiation. Arch. Biochem., Biophys. 50:322, 1954.

17. Tanford, C., and J. G. Buzzell. The viscosity of aqueous solutions of bovine serum albumin between pH 4.3 and 10.5. J. Phys. Chem. 60:225, 1956.

18. Taylor, G. I. Fluid friction between rotating cylinders, I Torque measurements. Proc. Roy. Soc. (London), A157:546, 1936.

19. Tirrell, M. and S. Middleman. Shear modification of enzyme kinetics. Biotech. Bioeng. 17:299, 1975.

20. Tirrell, M., and S. Middleman. Symposium on biorheology. AIChE Symposium Series. 1977.

21. Tirrell, M. and S. Middleman. Shear deformation effects on enzyme catalysis: Preliminary experimental results on lactic dehydrogenase. Biotech. Bioeng. 20:605, 1978.

22. Tirrell, M. Stress-induced structure and activity changes in biologically active proteins. J. Bioeng. 2:183, 1978.

23. Tirrell, M. and S. Middleman. Shear deformation effects on enzyme catalysis. Metal ion effect in the shear inactivation or urease. Biophys. J. 23:121, 1978.

24. Uhl, V. W., and J. B. Gray, Mixing: Theory and practice, Vol. II, Academic Press, New York, 1967.

APPENDICES

APPENDIX A

TABULATED DATA

APPENDIX A

TABULATED DATA

Table 4. Torque measurements

N(RPM)	w(g)	T_q(dyne cm) x 10^{-3}
100	11.26	28.02
150	15.13	37.66
200	20.41	50.80
250	26.40	65.69
300	46.81	116.5
350	67.22	167.3
400	88.34	219.9
450	111.56	277.7
500	134.44	334.6

Table 4. (Continued)

Stirred tank		T_q(dyne cm) x 10^{-3}	
N(RPM)	ν = 0.00412 cm^2/sec	ν = 0.01002 cm^2/sec	ν = 0.01307 cm^2/sec
500	34.4	46.1	47.2
1000	67.8	85.4	93.5
1500	103.2	139.	144.
2000	136.6	183.	179.
2500	175.3	222.	225.
3000	226.4	291.	287.

Table 5. Catalase adsorption to viscometer

[C] = 5 μg/ml	T = 1°C	
t(min)	$-k(sec^{-1})$ x 10^3	k/k_o
0	7.91	1.000
10	7.21	0.912
20	6.72	0.849
39	5.68	0.719
70	4.91	0.621
114	4.19	0.530
164	3.89	0.492
216	3.64	0.461
272	3.42	0.433
300	3.75	0.475

Table 5. (Continued)

$[C]$ = 5 μg/ml	T = 10°C	
t(min)	$-k(sec^{-1}) \times 10^3$	k/k_o
0	7.64	1.000
31	3.82	0.500
58	3.61	0.473
89	2.49	0.326
124	2.54	0.332
159	2.50	0.327
183	2.50	0.327
243*	3.73*	0.487*

*after 1.0 hour of shear at 1854 sec^{-1}

$[C]$ = 10 μg/ml	T = 1°C	
t(min)	$-k(sec^{-1})$ c 10^3	k/k_o
0	18.45	1.000
18	15.72	0.848
32	14.63	0.789
48	13.48	0.727
62	12.98	0.700
92	11.75	0.634
121	11.33	0.611
155	10.53	0.568
192	10.55	0.569
211	10.07	0.543
241*	10.50*	0.566*
287*	10.82*	0.584*

*shear rate = 1854 sec^{-1}

58

Table 6. Boehringer-Mannheim catalase, viscometer degradation.

$[C] = 5\ \mu g/ml$ $[A] = 0$ $T = 4°C$

$s = 0\ sec^{-1}$	$S_v = -0.47 \times 10^{-6}\ sec^{-1}$	$k_o = 9.25\ sec^{-1}$
$t(sec)$	$-k(sec^{-1}) \times 10^3$	k/k_o
0	9.37	1.013
2400	9.25	1.000
6000	9.03	0.977
9600	9.86	1.066
11400	9.43	1.020

$s = 618\ sec^{-1}$	$S_v = 4.22 \times 10^{-6}\ sec^{-1}$	$k_o = 11.32\ sec^{-1}$
$t(sec)$	$-k(sec^{-1}) \times 10^3$	k/k_o
0	11.39	1.006
1800	11.38	1.006
3600	10.62	0.938
5437	11.27	0.996
7200	11.24	0.993
9000	10.75	0.950

Table 6. (Continued)

$s = 1236$ sec^{-1}	$S_v = 5.25 \times 10^{-6}$ sec^{-1}	$k_o = 6.62$ sec^{-1}
t(sec)	$-k$(sec^{-1}) $\times 10^3$	k/k_o
0	6.75	1.019
1600	6.47	0.978
4100	6.47	0.977
6000	6.34	0.958
7500	6.33	0.955
9600	6.40	0.966
$s = 1854$ sec^{-1}	$S_v = 9.87 \times 10^{-6}$ sec^{-1}	$k_o = 9.09$ sec^{-1}
t(sec)	$-k$(sec^{-1}) $\times 10^3$	k/k_o
0	9.17	1.009
1800	8.82	0.970
3600	8.90	0.979
5400	8.50	0.935
7200	8.42	0.926
9000	8.40	0.924

Table 7.   Worthington catalase, viscometer degradation.

[C] = 5 μg/ml   [A] = 500 μg/ml   T = 2°C

s = 0 sec^{-1}	S_V = 0.11 x 10^{-6} sec^{-1}	k_o = 10.51 sec^{-1}
t(sec)	-k(sec^{-1}) x 10^3	k/k_o
0	10.52	1.001
3600	10.38	0.987
7290	10.79	1.026
10800	10.31	0.981
14460	10.53	1.002
s = 1236 sec^{-1}	S_V = 3.66 x 10^{-6} sec^{-1}	k_o = 12.38 sec^{-1}
t(sec)	-k(sec^{-1}) x 10^3	k/k_o
0	12.55	1.014
3600	12.05	0.974
7200	11.89	0.961
10800	12.06	0.974
s = 1854 sec^{-1}	S_V = 8.39 x 10^{-6} sec^{-1}	k_o = 8.72 sec^{-1}
t(sec)	-k(sec^{-1}) x 10^3	k/k_o
0	8.83	1.013
3700	8.47	0.972
7300	8.14	0.933
11360	7.80	0.895
14400	7.68	0.881
18000	7.49	0.859
21600	7.38	0.847

Table 8. Worthington catalase, viscometer degradation.

$[C] = 5$ µg/ml $[A] = 500$ µg/ml $T = 10°C$

$s = 0$ sec^{-1}	$S_v = 1.79 \times 10^{-6}$ sec^{-1}	$k_o = 6.69$ sec^{-1}
t(sec)	$-k$(sec^{-1}) $\times 10^3$	k/k_o
0	6.64	0.993
1860	6.73	1.007
3900	6.70	1.002
5820	6.54	0.978
8280	6.68	0.999
10140	6.49	0.971
12000	6.53	0.977
13380	6.69	1.000
14400	6.32	0.945
15720	6.35	0.950
18000	6.67	0.997

$s = 618$ sec^{-1}	$S_v = 4.99 \times 10^{-6}$ sec^{-1}	$k_o = 7.29$ sec^{-1}
t(sec)	$-k$(sec^{-1}) $\times 10^3$	k/k_o
0	7.25	0.994
1890	7.38	1.013
3960	7.14	0.979
5530	6.99	0.960
7400	6.88	0.944
9030	7.03	0.964
10800	6.98	0.957

Table 8. (Continued)

$s = 1297 \ sec^{-1}$	$S_v = 7.16 \times 10^{-6} \ sec^{-1}$	$k_o = 7.23 \ sec^{-1}$
$t(sec)$	$-k(sec^{-1}) \times 10^3$	k/k_o
0	7.44	1.028
990	7.57	1.046
2625	7.01	0.970
4900	6.85	0.948
6480	6.69	0.924
8215	6.38	0.883
9960	6.59	0.912
11700	6.68	0.924
13500	6.61	0.914
15200	6.87	0.951

$s = 1854 \ sec^{-1}$	$S_v = 11.48 \times 10^{-6} \ sec^{-1}$	$k_o = 7.72 \ sec^{-1}$
$t(sec)$	$-k(sec^{-1}) \times 10^3$	k/k_o
0	8.03	1.039
1870	7.51	0.972
3600	7.19	0.930
5470	7.21	0.934
7200	7.33	0.949
9400	6.62	0.858
11010	6.69	0.867
12630	6.55	0.849
14400	6.88	0.891
14400	6.57	0.851

Table 9.   Worthington catalase, viscometer degradation.

[C] = 5 μg/ml   [A] = 500 μg/ml   T = 20°C

s = 0 sec^{-1}	S_v = 2.22 x 10^{-6} sec^{-1}	k_o = 11.86 sec^{-1}
t(sec)	-k(sec^{-1}) x 10^3	k/k_o
0	12.17	1.026
1680	11.66	0.983
3480	12.04	1.015
5340	11.51	0.971
7200	11.66	0.982
8940	11.49	0.969
10800	11.31	0.953
12600	11.41	0.962
14400	11.58	0.976
10860	11.57	0.975
19500	11.47	0.967

s = 1152 sec^{-1}	S_v = 8.58 x 10^{-6} sec^{-1}	k_o = 13.72 sec^{-1}
t(sec)	-k(sec^{-1}) x 10^3	k/k_o
0	13.59	0.991
1800	13.69	0.998
3600	13.36	0.974
5400	12.94	0.943
7200	12.93	0.943
9000	12.71	0.926
9909	12.68	0.924
10800	12.44	0.907

Table 9. (Continued)

$s = 1728 \text{ sec}^{-1}$	$S_v = 1263 \times 10^{-6} \text{ sec}^{-1}$	$k_o = 9.53 \text{ sec}^{-1}$
$t(\text{sec})$	$-k(\text{sec}^{-1}) \times 10^3$	k/k_o
0	10.02	1.052
1800	9.00	0.945
3600	8.89	0.933
5400	8.98	0.943
7200	8.42	0.884
9000	8.49	0.891
10800	8.58	0.901

$s = 1854 \text{ sec}^{-1}$	$S_v = 13.13 \times 10^{-6} \text{ sec}^{-1}$	$k_o = 7.81 \text{ sec}^{-1}$
$t(\text{sec})$	$-k(\text{sec}^{-1}) \times 10^3$	k/k_o
0	8.36	1.071
2090	7.50	0.960
3860	7.07	0.906
5400	7.01	0.898
7200	7.08	0.907
9015	6.75	0.865
11490	7.12	0.912

Table 10. Worthington catalase, stirred tank degradation

[C] = 5 μg/ml   T = 1°C

N = 0 RPM	$S_t = -0.12 \times 10^{-4}$ min^{-1}	$k_o = 10.41$ sec^{-1}
t(min)	$-k(\text{sec}^{-1}) \times 10^3$	k/k_o
6.7	10.42	1.001
36.7	10.49	1.008
49.3	10.47	1.006
65.8	10.34	0.993
95.3	10.32	0.992
128.0	10.29	0.989
155.7	10.51	1.010
184.8	10.29	0.989
216.3	10.72	1.030
253.3	10.35	0.994
300.0	10.60	1.018
330.8	10.49	1.008
360.0	10.29	0.989
N = 1500 RPM	$S_t = 5.38 \times 10^{-4}$ min^{-1}	$k_o = 9.49$ sec^{-1}
t(min)	$-k(\text{sec}^{-1}) \times 10^3$	k/k_o
0.0	9.84	1.037
0.0	9.82	1.035
0.0	9.38	0.989
30.0	9.06	0.955
60.0	9.04	0.953
90.0	8.78	0.925
120.0	8.69	0.916
151.0	8.86	0.933
181.7	8.65	0.912
210.0	8.65	0.912

Table 10. (Continued)

N = 2250	$S_t = 10.37 \times 10^{-4} \text{ min}^{-1}$	$k_o = 10.41 \text{ sec}^{-1}$
t(min)	$-k(\text{sec}^{-1}) \times 10^3$	k/k_o
0.0	10.46	1.005
0.0	10.28	0.988
0.0	10.22	0.982
30.0	9.88	0.949
60.0	9.94	0.955
91.7	9.64	0.926
120.0	9.22	0.886
150.0	9.11	0.875
180.0	8.92	0.857
210.0	8.53	0.819
240.0	7.89	0.758
242.2	7.81	0.750

N = 3000 RPM	$S_t = 21.30 \times 10^{-4} \text{ min}^{-1}$	$k_o = 9.69 \text{ sec}^{-1}$
t(min)	$-k(\text{sec}^{-1}) \times 10^3$	k/k_o
0.0	9.48	0.978
0.0	9.54	0.984
0.0	9.30	0.960
31.0	9.22	0.951
60.0	8.88	0.916
93.3	8.41	0.867
121.0	7.56	0.780
150.0	7.03	0.725
180.0	6.56	0.677
210.0	6.14	0.633
240.0	5.67	0.585

Table 10. (Continued)

N = 3000 RPM	$S_t = 12.05 \times 10^{-4} \min^{-1}$	$k_o = 9.54 \sec^{-1}$
t(min)	$-k(\sec^{-1}) \times 10^3$	k/k_o
0.0	9.58	1.004
0.0	9.58	1.005
0.0	9.72	1.019
30.0	9.20	0.965
90.0	8.23	0.863
121.7	8.17	0.856
150.0	7.76	0.814
181.7	7.96	0.835
212.2	7.43	0.779

$S_t = 16.68 \times 10^{-4} \min^{-1}$ (combined 3000 RPM data)

Table 11.   Worthington catalase, stirred tank degradation.

[C] = 5 μg/ml   T = 10°C

N = 0 RPM	$S_t = 0.25 \times 10^{-4} \text{ min}^{-1}$	$k_o = 6.59 \text{ sec}^{-1}$
t(min)	$-k(\text{sec}^{-1}) \times 10^3$	k/k_o
0.0	6.52	0.989
31.0	6.76	1.025
65.0	6.55	0.995
98.0	6.95	1.054
127.0	6.01	0.912
155.0	6.65	1.009
193.0	6.78	0.968
213.0	6.65	1.010
245.0	6.70	1.017
N = 1000 RPM	$S_t = 5.59 \times 10^{-4} \text{ min}^{-1}$	$k_o = 6.35 \text{ sec}^{-1}$
t(min)	$-k(\text{sec}^{-1}) \times 10^3$	k/k_o
0.0	6.38	1.005
30.0	6.32	0.996
60.0	6.00	0.945
90.0	6.05	0.954
120.0	5.88	0.926
150.0	5.88	0.926
180.0	5.81	0.915
210.0	5.59	0.880
240.0	5.57	0.877

Table 11. (Continued)

N = 1500 RPM	$S_t = 8.21 \times 10^{-4} \text{ min}^{-1}$	$k_o = 7.46 \text{ sec}^{-1}$
t(min)	$-k(\text{sec}^{-1}) \times 10^3$	k/k_o
0.0	7.38	0.989
32.0	7.26	0.973
62.0	7.13	0.956
94.0	7.01	0.939
120.0	6.79	0.910
150.0	6.64	0.889
180.0	6.33	0.848
210.0	6.26	0.839
240.0	6.15	0.823

N = 2000 RPM	$S_t = 14.02 \times 10^{-4} \text{ min}^{-1}$	$k_o = 6.86 \text{ sec}^{-1}$
t(min)	$-k(\text{sec}^{-1}) \times 10^3$	k/k_o
0.0	7.01	1.022
30.0	6.61	0.964
61.0	6.07	0.885
91.7	5.92	0.863
121.7	5.91	0.862
151.7	5.51	0.804
180.0	5.39	0.786
210.0	5.15	0.751
240.0	4.87	0.710

Table 11. (Continued)

N = 2500 RPM	S_t = 17.89 x 10^{-4} min^{-1}	k_o = 7.81 sec^{-1}
t(min)	$-k(sec^{-1})$ x 10^3	k/k_o
0.0	7.60	0.973
30.0	7.70	0.986
60.0	6.85	0.976
90.0	6.65	0.851
122.7	6.41	0.821
151.5	5.98	0.766
181.0	5.64	0.721
212.2	5.36	0.686
240.0	5.02	0.643

N = 3000 RPM	S_t = 16.32 x 10^{-4} min^{-1}	k_o = 6.73 sec^{-1}
t(min)	$-k(sec^{-1})$ x 10^3	k/k_o
0.0	6.59	0.979
30.0	6.40	0.951
60.0	6.09	0.905
90.0	5.97	0.887
120.0	5.95	0.884
150.0	4.91	0.729
180.0	5.03	0.747
210.0	4.67	0.694
258.3	4.48	0.666

Table 11. (Continued)

N = 3000 RPM	$S_t = 27.11 \times 10^{-4} \, min^{-1}$	$k_o = 5.48 \, sec^{-1}$
t(min)	$-k(sec^{-1}) \times 10^3$	k/k_o
0.0	5.50	1.004
5.3	5.74	1.046
31.0	5.06	0.924
60.0	4.75	0.866
90.5	4.14	0.756
121.0	3.75	0.685
150.0	3.39	0.618
182.7	3.31	0.604
218.0	2.96	0.539
240.0	3.20	0.583

$$S_t = 21.72 \times 10^{-4} \, min^{-1} \text{ (combined 3000 RPM data)}$$

Table 12. Worthington catalase, stirred tank degradation.

[C] = 5 µg/ml   T = 20°C

N = 0 RPM	$S_t = 0.55 \times 10^{-4} \text{ min}^{-1}$	$k_o = 8.05 \text{ sec}^{-1}$
t(min)	$-k(\text{sec}^{-1}) \times 10^3$	k/k_o
0.0	8.11	1.006
71.0	7.94	0.986
102.0	7.99	0.992
127.0	8.12	1.009
160.0	8.03	0.996
178.0	7.78	0.966
240.0	8.04	0.998
N = 1000 RPM	$S_t = 6.40 \times 10^{-4} \text{ min}^{-1}$	$k_o = 7.37 \text{ sec}^{-1}$
t(min)	$-k(\text{sec}^{-1}) \times 10^3$	k/k_o
30.0	7.40	1.004
60.0	7.03	0.954
90.0	6.84	0.928
124.8	6.81	0.925
151.5	6.58	0.894
180.0	6.56	0.890
211.0	6.55	0.889

Table 12. (Continued)

N = 1500 RPM	S_t = 14.55 x 10^{-4} min^{-1}	k_o = 7.76 sec^{-1}
t(min)	$-k(sec^{-1})$ x 10^3	k/k_o
0.0	8.01	1.033
31.0	7.49	0.966
60.0	6.77	0.873
91.0	6.91	0.891
121.5	6.38	0.822
150.0	6.19	0.797
180.0	5.96	0.768
210.0	5.61	0.723
247.2	5.61	0.724

N = 2000 RPM	S_t = 16.93 x 10^{-4} min^{-1}	k_o = 8.13 sec^{-1}
t(min)	$-k(sec^{-1})$ x 10^3	k/k_o
0.0	8.16	1.004
30.0	7.75	0.953
60.0	7.19	0.885
90.0	6.89	0.848
121.7	6.82	0.839
159.7	6.38	0.785
180.0	5.85	0.720
210.0	5.59	0.688
240.0	5.46	0.672

Table 12. (Continued)

N = 2500 RPM	$S_t = 22.61 \times 10^{-4} \text{ min}^{-1}$	$k_o = 7.78 \text{ sec}^{-1}$
t(min)	$-k(\text{sec}^{-1}) \times 10^3$	k/k_o
0.0	7.94	1.020
30.0	6.76	0.868
62.2	6.78	0.871
91.0	6.73	0.864
121.0	6.09	0.783
150.0	5.57	0.716
181.0	4.95	0.636
210.0	4.83	0.620
240.0	4.54	0.583

N = 3000 RPM	$S_t = 28.44 \times 10^{-4} \text{ min}^{-1}$	$k_o = 8.11 \text{ sec}^{-1}$
t(min)	$-k(\text{sec}^{-1}) \times 10^3$	k/k_o
0.0	4.50	0.924
0.0	8.78	1.082
30.0	7.44	0.917
35.0	7.59	0.936
60.0	6.76	0.833
90.0	6.34	0.781
120.0	5.81	0.716
155.0	5.05	0.623
185.5	4.59	0.566
246.0	4.36	0.537

APPENDIX B

ASSAY COMPUTER PROGRAM

APPENDIX B

ASSAY COMPUTER PROGRAM

```
C     AR = THE ABSORBANCE VECTOR
C     T  = THE TIME VECTOR
C     INT = THE TIME INTERVAL IN MILLISECONDS, NEGATIVE
C           THE TIME AFTER INJECTION WHEN THE FIRST POINT IS READ
C     TEND = THE TIME WHEN THE LAST POINT IS READ
C     VMIN = THE MINIMUM VOLTAGE ACCEPTED IN OD
C     NI = THE NUMBER OF POINTS AVERAGED IN OD
C     NAME = THE TYPE OF ENZYME
C     DT = INT/-1000 = THE TIME INTERVAL IN SECONDS
C     NUM = THE MAXIMUM NUMBER OF DATA POINTS READ
C     SLOPE = THE RATE CONSTANT
C     YO = THE ABSORBANCE AT T=0
C     R2 = A GOODNESS OF FIT PARAMETER
C     ICN = DATA POINT INDEX
C     NS = THE SIGNAL TO READ DATA
C     IDTSW(I) = EXTERNAL SWITCHES
C     HYADR = ANALOG OUTPUT, WHICH LIGHTS A LED WHEN COMPUTER IS READY

      EXTERNAL OD
      DIMENSION IDATE(3), NAME(20), Y(25), X(25), T(500), S(50)
      COMMON IFLAG, I, NUM, AB(500), NI
      DATA SX, SY, R2, SLOPE, YO/ 5*0.0/
      CL = 20.

C     CALCULATE DT AND DELAY PARAMETER ITIME
      READ(2,202) INT,TIME,TEND,VMIN,NI, (NAME(K),K=1,20)
      DT = FLOAT(INT)/(-1000.)
      UM = (1./DT)*(TEND-TIME) + 1
      NUM = IFIX(UM)
      ITIME = IFIX(TIME)*4000
      CALL HYADR(30, 0.0)

C     READ AND PRINT CONDITIONS
      WRITE(1,210)
      READ(6,212) IDATE(1), IDATE(2), IDATE(3)
      WRITE(3,210) (IDATE(K),K=1,3), (NAME(J),J=1,20)
      WRITE(3,201) DT, TIME, TEND
      WRITE(3,216) NI, VMIN
      WRITE(3,207)
```

```fortran
C     INITIALIZE THE TIME VECTOR
      DO 5 J=1,NUM
      T(J) = TIME
    5 TIME = TIME + DT
      ICN = 0
C
C     CHECK SIGNAL UNTIL A PULSE IS OBSERVED, OR EXIT IF IDTSW(1) IS ON.
    9 SUM = 0.
   10 CALL HYADR(30, 0.202)
      IF(IDTSW(1)-1) 1, 1, NS)
   13 IF(IDTSW(1)-1) 13, 90, 90
   14 IF(8000 + NS) 15, 15, 10
C
C     CALL OD EVERY DT SECONDS UNTIL VECTOR AB IS FILLED.
   15 T = 0
      CALL HYADR(30, 0.0)
      ICN = ICN + 1
      IFLAG = 1
      CALL HYDLY(ITIME)
      CALL INTMR(OD, 2, INT)
   20 IF(I, 23, 23, 21
   21 IF(AB(I) - VMIN) 25,23,23
   23 GO TO (20,25) IFLAG
   25 CALL INTMR(OD, 2,-INT)
C
C     PLOT ABSORRANCE V.S. TIME
      XSC = 2./TEND
      CALL HYPLT(0.,0.,0.)
      CALL HYPLT(XSC, 1.0, 3)
      CALL HYPLT(0.,6.,1)
      CALL HYPLT(T(1), AB(1), 2)
      DO 30 J=1, I
      CALL HYPLT(T(J), AB(J), 1)
      IF(IDTSW(2)-1) 30, 28, 28
   28 WRITE(3,202) J, T(J), AB(J)
   30 AB(J) = ALOG(AB(J))
C
```

```fortran
C     CALCULATE AND PRINT RATE CONSTANT
      CALL HYPLT(T(I), 0.,2)
      S(ICN) = SLOPE
      YO = EXP(YO)
      WRITE(1,203) ICN, YO, SLOPE, R2
      WRITE(3,203) ICN, YO, SLOPE, R2
      WRITE(3,203) ICN, YO, SLOPE, R2
      GO TO 9
C
  201 FORMAT(//,5X,' DT =',F7.3,' SECONDS',//,5X,'T(I) =',F6.2,
     1' SECONDS',' 10X,'T(F) =',F6.1,' SECONDS',' 14, 20A1)
  202 FORMAT(I8, F12.3, F13.4, F5.2, I4, 20A1)
  203 FORMAT(I4, F11.3, E15.4, F10.4,/)
  207 FORMAT(//,5X,'SWITCH(0) = ON ',/,5X,'SWITCH(1) = CONTINUE   ',/,
     15X,'SWITCH(2) = LIST DATA',/,5X,'SWITCH(3) = SIGNAL  ',/,
     25X,'SWITCH(4) = ABORT',/,9X,'THETA',6X,'K (1/SEC)',/ )
  208 FORMAT(1H1,/,9X,'THETA',6X,'K (1/SEC)',/ )
  210 FORMAT(/,' DATE', 3I3, 42X, 20A1)
  212 FORMAT(3I2)
  213 FORMAT(//,4X,'SLOPE =',E12.5,6X,'F(0) =',E12.5,6X,'R2 =',F8.5,//)
  214 FORMAT(//,4X,'NORMALIZED SLOPE =',E12.5,//)
  216 FORMAT(//,5X,'AVERAGE =',I4,' TIMES',10X,'MINIMUM VOLTAGE =', F6.3,//)
  217 FORMAT(1H1,/,14X,'THETA',10X,'K/KO',/)
  218 FORMAT(F8.1)
C
C     READ EXPOSURE TIMES
   90 WRITE(3,208)
      CALL HYADR(30, 0.0)
      DO 100 J=1, ICN
      WRITE(1,202) J
      READ(6, 218) ET
      T(J) = ET/60.
      WRITE(3,203) J, T(J), S(J)
      WRITE(3,203)
  100 CONTINUE
```

```
C
C     DISCARD IRRELEVANT DATA POINTS
      INDEX = 0
      DO 98 J=1,ICN
      IF(T(J)) 98, 92, 92
   92 INDEX = INDEX + 1
      Y(INDEX) = S(J)
      X(INDEX) = T(J)
   98 CONTINUE
C
C     CALCULATE AND PRINT SLOPE OF RATE CONSTANT V.S. EXPOSURE TIME
      CALL LST2(INDEX, Y, X, SLOPE, YO, R2)
      WRITE(3,213) SLOPE, YO, R2
      SLOPE = SLOPE/YO
      WRITE(3,214) SLOPE
C
C     NORMALIZE RATE CONSTANTS AND GRAPH DATA
      WRITE(3,217)
      READ(6,202) L
      CALL P7540(SX, SY, CL, L)
      DO 110 J=1,INDEX
      Y(J) = Y(J)/YO
      CALL PLOTP(1, X(J), Y(J), SX, SY)
      WRITE(3,202) J, X(J), Y(J)
      WRITE(3,203)
  110 CONTINUE
      CALL PLOT3(0.0, 300.0, SLOPE, 1.)
      IF(IDTSW(4)-1) 90, 150, 150
C
C     ITPEX RESETS THE INTERVAL TIMERS
  150 WRITE(3,217)
      CALL HYPLT(0.,0.,-1)
      CALL ITPFX
      CALL EXIT
      END
```

```
C     OD IS THE DATA GATHERING SUBROUTINE
C     DATA IS READ N1 TIMES AND AVERAGED
C     WHEN IFLAG IS 2, THE VECTOR AB IS FILLED

      SUBROUTINE OD
      COMMON IFLAG, I, NUM, AB(500), N1
      I = I+1
      SUM = 0.0
      DO 9 J=1, N1
      CALL HEAIR(12, 1, A)
      SUM = SUM + A
    9 CONTINUE
      AB(I) = SUM/N1
      IF(NUM-I) 20,20,25
   20 IFLAG = 2
   25 CONTINUE
      RETURN
      END
```